UNIVERSITA DEL PIEMONTE ORIENTALE

Via Solaroli 17, Novara-28100,Italy

PHD PROGRAM CYCLE XXXIV YEAR:
2018-2021

"Macrophage Phenotype during Liver Injury and Repair."

Patologia Generale

Coordinator:

Prof.Marisa Garilio

Mentor:

Prof. Emanuele Albano

Student
Laila Lavanya Gadipudi

Table Content

General Abstract

Growing evidence indicates that the activation of liver resident macrophages, known as Kupffer cells, along the recruitment of monocyte-derived macrophages (MoMFs) plays and important role during the evolution of acute and chronic liver damage. A key aspect in this field concerns the characterization of the signals that contribute to modulate the great functional plasticity of hepatic macrophages in the switching from pro-inflammatory to repair functions as well as in promoting the liver disease progression to fibrosis/cirrhosis. This doctoral project has investigated some of these aspects focalizing on:

a) The role of the lymphocyte co-stimulatory molecule Inducible T-cell Costimulator (ICOS) in modulating macrophage functions during liver repair following an acute injury.

b) The capacity of the anti-inflammatory mediator Annexin A1 of influencing the pro-fibrogenic action of macrophages during the evolution of chronic liver damage in an experimental nonalcoholic steatohepatitis (NASH).

The first study investigated the contribution of the interaction between T-lymphocytes and MoMFs through the co-stimulatory molecule Inducible T-cell co-stimulator (ICOS; CD278) and its ligand (ICOSL; CD275) in modulating liver recovery from acute liver damage induced by a single dose of carbon tetrachloride (CCl_4). Using flow cytometry of non-parenchymal liver cells obtained from CCl_4-treated wild-type mice we observed that the recovery from acute liver injury associated with a specific up-regulation of ICOS in $CD8^+$ T-lymphocytes and with an increase in ICOSL expression involving $CD11b^{high}/F4\text{-}80^+$ hepatic MoMFs. Although ICOS deficiency did not influence the severity of liver damage and the evolution of inflammation, CCl_4-treated in ICOS knockout ($ICOS^{-/-}$) mice showed delayed clearance of liver necrosis and increased mortality. These animals were also characterized by a significant reduction of hepatic reparative MoMFs due to an increased rate of cell apoptosis. An impaired liver healing and loss of reparative MoMFs was similarly evident in ICOSL-deficient mice or following $CD8^+$ T-cells ablation in wild-type mice. The loss of reparative MoMFs was prevented by supplementing CCl_4-treated $ICOS^{-/-}$ mice with recombinant ICOS (ICOS-Fc) which also stimulated full recovery from liver injury. These data demonstrated that $CD8^+$ T-lymphocytes play a key role in supporting the survival of reparative MoMFs during liver healing trough ICOS/ICOSL-mediated signaling. These observations open the possibility of targeting ICOS/ICOSL dyad as a novel tool for promoting efficient healing following acute liver injury.

Annexin A1 (AnxA1) is an important effector in the resolution of inflammation and recent studies have shown its involvement in modulating hepatic inflammation in nonalcoholic steatohepatitis (NASH). In the second study we have investigated the effects of the treatment with human recombinant (hrAnxA1; 1µg, daily IP) in counteracting the progression of experimental NASH induced in C57BL/6 mice by feeding methionine-choline deficient (MCD) or Western diets. In both experimental models of NASH, we observed that the administration of hrAnxA1 improved parenchymal injury and lobular inflammation without interfering with the extension of steatosis. Furthermore, hrAnxA1 significantly attenuated the hepatic expression of α1-procollagen and TGF-ß1 and reduced collagen deposition, as evaluated by collagen Sirius Red staining. Flow cytometry and immunohistochemical analyses of liver mononuclear cells showed that hrAnxA1 did not affect the liver recruitment of MoMFs, but strongly interfered with the formation of crown-like MoMF aggregates and reduced their capacity of producing pro-fibrogenic mediators like osteopontin (OPN) and galectin-3 (Gal-3). This effect was related to an interference with the acquisition of a specific MoMF phenotype characterized by the expression of the Triggering Receptor Expressed on Myeloid cells 2 (TREM-2), CD9 and CD206, all previously associated with NASH evolution to cirrhosis. Altogether these results indicate that, beside ameliorating hepatic inflammation, AnxA1 is specifically effective in preventing NASH-associated fibrosis by interfering with pro-fibrogenic features of MoMFs. Such a novel function of AnxA1 gives the rational for the development of AnxA1 analogues for the therapeutic control of NASH evolution.

1. Introduction

1.1) Macrophages in Healthy Liver.

The liver is among all human organs the one which harbours the largest fraction (about 80-90%) of all the macrophages present in the body (Guilliams et al.2016). The hepatic macrophage pool consists of a heterogeneous population that involves self-renewing tissue-resident phagocytes, termed as Kupffer cells (KCs), and infiltrating macrophages that are derived from circulating monocytes originating from bone marrow resident hemopoietic stem cells (MoMFs) (Krenkel et al 2017). Kupffer cells account for 20-35% of all nonparenchymal liver cells. These cells were first described in 1876 by Wilhelm von Kupffer as "sternzellen" that is star or symmetric cells. Kupffer cells were initially thought to be a component of the endothelium of the liver blood vessels, however later in 1898, they were correctly identified as macrophages by Tadeusz Browiecz (Browiecz et al 1898). Although Kupffer cells localize within the liver, they do not actually reside within the parenchyma, but are intercalated in the liver sinusoids and by extending portion of the cell body get contact with hepatic stellate cells (HSCs) and hepatocytes (Ramachandran et al 2010). Kupffer cells are detectable throughout the liver, however, are less frequent in the immediate vicinity of the central vein (Introduction Fig I Krenkel et al 2017).

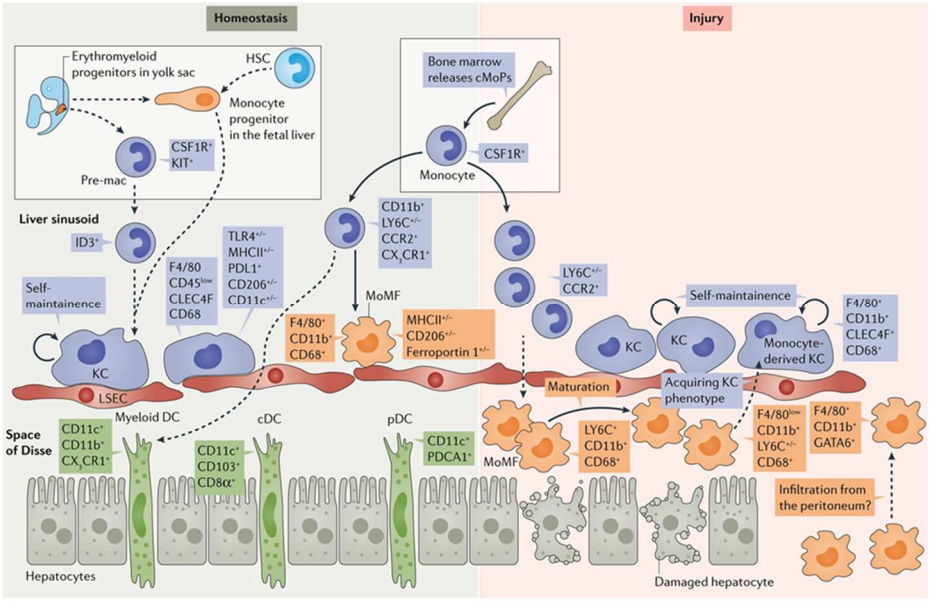

Introduction Figure I: Origin and features of hepatic macrophages (From Krenkel and Tacke 2017).

It is now well established that Kupffer cells are long-lived, with a half-live of about 12 days, and have the capacity of self-renewing, minimally relaying from the input of circulating monocytes (Yona et al. 2013; Gomez Perdiguero et al. 2015). In fact, Kupffer cells originate from the yolk sac erythromyeloid progenitor (EMPs) expressing the macrophage colony-stimulating factor 1 receptor (CSF1R; also known as CD115), that colonize the vertebrate liver around the 10-12 day of embryogenesis giving rise to fetal liver monocytes and subsequently mature macrophages (Gomez Perdiguero, et al. 2015). Nonetheless, there are evidence that in an earlier phase, at E8.5, yolk sac EMPs develop into circulating macrophage precursors (pre-macrophages), which migrate to the foetal liver before day 10.5 and subsequently differentiate to Kupffer cells through the action of the transcription factor, inhibitor of differentiation 3 (ID3) (Kim et al. 2016). In the healthy liver, Kupffer cells renewal relays on niche environment and is tightly controlled by specific transcription repressors and enhancers (Mass E et al. 2016). However, recent data points to the fact that in pathological conditions extensive loss of Kupffer cells can be repleted by circulating monocytes, suggesting that adult monocytes have the potential as their embryonic counterparts to turn into Kupffer cells (Soucie L et al. 2016).

Using immunohistochemistry Kupffer cells can be differentiated from other liver non-parenchymal cells by the expression of CD45 and the macrophage marker F4-80 in mice or CD68 in humans. They also express low or intermediate levels of the leukocyte integrin alfa M (ITGAM or CD11b) and lack the fractalkine receptor CX_3CR1, owing to their non-monocytic origin (Guilott and Tacke 2019). However, these markers are not specific as they also are shared by monocyte-derived macrophages (MoMFs) and this has led to some confusion in investigating the specific functions of these cells. More recent studies have revealed that, at least in the mouse, the C-type lectin domain family 4 member F (Clec4F) is a more specific marker of Kupffer cells and together with stabilin 2 (Stab2) and the T cell immunoglobulin and mucin domain containing 4 (Timd4) allow their better differentiation for MoMFs (Guilott and Tacke 2019). Human Kupffer cells are less well characterized and are tentatively identified by the positivity to CD14, CD68 and the scavenger receptor MARCO. These cells are also characterized by an enhanced expression of genes involved in down modulating immune responses and inflammation such as V-set and immunoglobulin domain containing 4 (VSIG4),

the haemoglobin-haptoglobin scavenger receptor, also known as CD163, and haemeoxygensase-1 (HMOX1) (Wen et al. 2021).

Healthy livers also contain a variable proportion of monocyte-derived macrophages which are more abundant in the portal triad (Gamella E et al 2014; Lopez B et al 2011). As Kupffer cells MoMFs are F4-80^{+}/CD11b^{+} but lack Clec4F and express the plasma membrane protein lymphocyte antigen 6 complex, locus C1 (Ly6C), previously termed Gr1, and class II Mayor Histocompatibility Cluster (MHCII) antigens (Yona et al. 2013). According to the intensity of Ly6C expression liver MoMFs can be distinct in Ly6C^{high} MoMFs, which directly derive from circulating monocytes and are short living (half-life of about 20 hours) and Ly6C$^{low/negative}$ MoMFs that derive from these latter (Yona et al. 2013). Ly6C$^{low/negative}$ MoMFs are self-renewing cells with a half-life of two days and represent the main pool of non-Kupffer cells macrophages within the liver (Yona et al. 2013). A particular sub-set of hepatic MoMFs involves those residing in the hepatic capsule. These liver capsular macrophages (LCMs) are CD11b^{+}/F4-80^{+}/MHC-II^{+}, but negative for Ly6C, Clec4F and TIM4, suggesting that they are distinct from Ly6C^{+} MoMFs and Kupffer cells, although they derive from circulating monocytes (Sierro et al. 2017). The main function of liver capsular macrophages is to clear peritoneal bacteria accessing the liver capsule and to promote the recruitment of neutrophils, thereby reducing hepatic pathogen loads (Sierro et al. 2017).

1.2) Functions of hepatic macrophages during homeostasis

The large number of macrophages present in the liver has raised many issues concerning their functions. Indeed, Kupffer cells play key actions in maintaining liver functions as well as in whole body homeostasis. Their main activities include: (a) the clearance of cellular debris and metabolic waste; (b) the control of iron homeostasis through the phagocytosis of erythrocytes and iron recycling; (c) the regulation of cholesterol homeostasis; (d) antimicrobial defence; (e) the induction of immune tolerance toward nutritional antigens (Wen et al. 2021) (Introduction Fig II).

Along with splenic macrophages Kupffer cells are essential in the clearance of damaged or aged erythrocytes. In fact, experiments using chromium-labelled red blood cells injected into

mice have shown that they are rapidly taken up nearly half of the injected cells. This process relies on the presence of scavenger receptors recognizing polyinosinic acid and phosphatidylserine (Terpstra and van Berkel 2000; Willekens et al 2005). Strictly associated with erythrocyte clearance is the capacity of Kupffer cells of the recycling iron derived from the degradation of hemoglobulin in order to maintain iron homeostasis. In this latter respect, Kupffer cells express genes involved in uptake, processing, and export of iron to hepatocytes (Scott and Guilliams 2018). In addition to the disposal of erythrocytes, Kupffer cells also contribute to the clearance of aged platelets which are mainly recognized by macrophage galactose lectin (Deppermann et al. 2020).

Growing evidence points to the importance of macrophages in regulating lipid metabolism (Remmerie and Scott 2018). Kupffer cells and alveolar macrophages are specifically enriched for lipid metabolism genes and significantly contribute to the uptake and degradation of modified and oxidized lipoproteins through the scavenger receptors CD36, LOX-1, SR-A1, and SR-B1 thus regulating cholesterol homeostasis (Remmerie and Scott 2018). Furthermore, Kupffer cells are responsible for the production of cholesteryl ester transfer protein, which is important for decreasing circulating high-density lipoprotein-cholesterol levels and increasing very low-density lipoprotein-cholesterol levels (Remmerie and Scott 2018).

Because their localization within the hepatic sinusoids Kupffer cells have direct contact with circulating pathogens and serve as the first-line defence against infections by efficiently recognizing and removing bacteria translocating from the gut (Bennett et al. 2021). In particular, by selectively expressing the receptors for the complement fragment C3b and iC3b are specifically effective in recognizing lipoteichoic acid (LTA) present in the capsule of Gram-positive bacteria (Helmy et al. 2006). Indeed, in mice after intravenous injection of bacteria more than 60% of them are trapped by the liver within 10 minutes, and the clearance reach more than 80% within 6 hours (Yang et al. 2014). In relation to their number and the extensive phagocytic activity Kupffer cells also represent the major population of antigen presenting cells (APCs) in the liver. However, their role in modulating immune responses mainly involves the maintenance of liver immunological tolerance (Doherty 2016). This action involves the activation of regulatory T cells (Tregs) producing IL-10 as well as the suppression of effector T-cell activation induced by other antigen presenting cells (You et al. 2008; Heymann et al. 2015) through the interaction between programmed cell death protein 1

(PD1) and PD1 ligand 1 (PDL1), or through the secretion of prostaglandin E2 (PGE2) and kinurenine (You et al. 2008; Yan et al. 2010).

1.3) Macrophage responses to liver injury

As mentioned above Kupffer cells have direct contact with sinusoidal blood and through their long cytoplasmic protrusions with other liver cells such as hepatocytes, hepatic stellated cells and endothelial cells. These interactions along with the rich variety of pattern recognition receptors (PRRs) present on their surface make Kupffer cells highly suitable to respond to a variety of stimuli related with liver injury (Guillot and Tacke 2019). Indeed, a plethora of signals associated with the initiation and progression of liver damage can cause Kupffer cell activation. Among the stimuli mainly responsible there are: (a) Damage signals released by various liver cells such as high mobility group box 1 (HMGB1), mitochondrial DNA (mtDNA), and ATP, reactive oxygen species (ROS) (Kubes and Mehal 2012) along with extracellular vesicles containing mitochondrial double-stranded RNA, microRNA (miRNA)-27 and heat shock protein 90 (HSP90) (Saha et al 2018; Lee et al 2020). (b) The presence of an excess of pathogen-associated molecular patterns (PAMPs) in the portal blood resulting from an increased intestinal permeability or changes in gut microbiota (Heymann and Tacke 2016). Nonetheless, recent data also suggest that metabolic changes caused by excessive uptake of dietary fats and carbohydrates as well as the increase in hepatic triglyceride and cholesterol content can similarly promote Kuppfer cell activation (Remmerie et al. 2020).

As a result, these stimuli Kuppfer cells activate a pro-inflammatory response consisting in the production of a great variety of mediators including cytokines, chemokines, prostaglandins, leukotrienes, ROS, nitrogen monoxide (NO) and granule enzymes (Introduction Fig. II). In particular, Kuppfer cells are a source of the chemokine CCL2 which recruits to the liver monocytes expressing the CCR2 receptor (Fig. 1) and secrete CXCL1, CXCL2, and CXCL8 to attract neutrophils (Wen et al. 2021). The recruitment of monocytes in responsible for the rapid increase in the fraction of Ly6C^{high} MoMFs that characterize diseased livers (Krenkel and Tacke 2017). Indeed, interference with CCL2/CCR2 signalling effectively reduces MoMF liver infiltration in response to hepatic damage (Krenkel and Tacke 2017). Activated Kupffer cells and MoMFs also release CCL5, CXCL9 and CXCL16 leading to the hepatic recruitment of,

respectively, $CD4^+$ and $CD8^+$ T and natural killer T-cells (NKT), which further contribute to sustain inflammatory and immune responses (Wen et al. 2021; Sutti and Albano 2020). Current view indicates that in mice circulating monocytes consist of two populations that are differentiated by their expression of Ly6C and fractalkine (CX3CL1) receptor CX3CR1 in $CX3CR1^{low}/CCR2^+/Ly6C^{high}$ and $CX3CR1^{high}/CCR2^-/Ly6C^{low}$ subsets. The former are immature cells mainly involved in inflammatory activity, while the $CX3CR1^{high}$ mature subset has the ability to differentiate toward macrophages or dendritic cells (Krenkel and Tacke 2017). In humans the same cells are characterized as $CX3CR1^{low}/CD14^+/CD11b^{high}/CD16^-$ or $CX3CR1^{high}/CD14^{low}/ CD16^+/CD11b^+$ respectively (Geissmann et al. 2003; Liu K et al 2009). Pro-inflammatory $Ly6C^+$ MoMFs have also been proposed to derive from $CX3CR1^{low}/CCR2^+/Ly6C^{high}$ monocytes. Nonetheless, these latter are also the precursors of $Ly6C^-$ MoMFs (Yona et al. 2013). Liver recruited MoMFs substantially contribute to the production of pro-inflammatory mediators since as compared with Kupffer cells, $Ly6C^{high}$ MoMFs produce higher levels of cytokines, complement factors, and have a marked proinflammatory phenotype (Mossanen et al. 2016) characterized by the expression of high levels of T-cell Ig mucin 3 (Havcr2), toll-like receptor-2 (TLR-2), the C-type lectins Clec4d, Clec4e, adhesion molecule 3 (ICAM3) and the complement C1q receptor CD93 (Zigmond et al 2016). Beside circulating monocytes an additional source for hepatic macrophages might be represented by peritoneal macrophages, which can be recruited through the visceral endothelium into liver parenchyma. Studies in mice have in fact demonstrated that mature peritoneal macrophages expressing the intercellular adhesion molecule 2 (ICAM2; CD102) and the transcriptional regulator GATA Binding Protein 6 (GATA6) migrate toward subcapsular liver tissue within one hour after sterile injury and that macrophage recruitment and tissue regeneration is impaired in GATA6-deficient mice (Wang and Kubes 2016).

As compared to mice the characterization of liver infiltrating MoMFs in humans is less well defined. Earlier studies have shown an increased prevalence of $CD14^+/CD16^+$ hepatic macrophages in patients with chronic liver diseases which associate with a high phagocytic activity, and the secretion of pro-inflammatory and fibrogenic mediators (Liaskou et al. 2013). More recent data indicates that human $CD68^+/MARCO^-$ macrophages have a similar transcriptional profile as recruited proinflammatory macrophages detected in rodent livers (MacParland et al. 2018).

The hepatic infiltration by MoMFs is also important to replace the loss of Kupffer cells caused by infection with DNA-encoding viruses or the bacterium Listeria monocytogenes, but that often accompanies also hepatocyte killing by toxins or during steatohepatitis (Wen et al. 2021). Indeed, after selective depletion of Clec4F-expressing Kupffer cells, recruited MoMFs fully replace them within 1 month (Beattie et al. 2016). However, recent data obtained by using a novel mouse model of selective Kupffer cells depletion, have shown that monocytes can acquire a "Kupffer cells phenotype" within days. This process depends on direct interaction with hepatic stellate cells (HSCs) and liver sinusoid endothelial cells (LSECs), which promotes monocyte differentiation to Kupffer cells through the action of the transcription factors ID3 and liver X receptor-alpha (LXR-α) (Bonnardel et al. 2019; Sakai et al. 2019). Such a colonization of Kupffer cell niche by liver infiltrating MoMFs greatly complicate the task of differentiating the functions of these two macrophages populations in response to hepatic damage, particularly during chronic liver diseases (Guillot and Tacke 2019).

1.4) Role of hepatic macrophages in the evolution of acute liver injury

A large body of experimental studies in which acute liver injury was induced in mice by carbon tetrachloride, concanavalin A, ischaemia–reperfusion, viral infections or sterile heat injury have shown that hepatic macrophages have a common response to acute liver damage, although some of the molecular pathways that activate macrophages might differ between the types of injury (Krenkel and Tacke 2017). Kupffer cells are the sensors of initial tissue damage and, as mentioned above, their activation leads to the release of pro-inflammatory mediators as well as to hepatic recruitment of pro-inflammatory monocytes, which mature into MoMFs (Krenkel and Tacke 2017). However, beside Kupffer cells, hepatic stellate cells, liver sinusoidal endothelial cells and hepatocytes are also sources of the chemokines involved in promoting liver monocyte infiltration (Marra and Tacke 2014). Colony stimulating factor 1 (CSF1) is an additional mediator of liver MoMF infiltration since it favours monocyte survival along with the proliferation of liver-resident macrophages (Stutchfield et al. 2015). Infiltrating Ly6C$^+$ MoMFs are highly plastic and in mouse models of acute liver damage can have both pro-inflammatory and anti-inflammatory functions. For instance, after acetaminophen-induced liver injury, newly infiltrated Ly6C$^+$ MoMFs significantly contribute

to liver damage and in humans, a high prevalence of circulating monocytes associates to a greater severity of liver failure and reduced survival of patients with acetaminophen poisoning (Jaeschke and Ramachandran 2020). The signal pathways responsible for the pro-inflammatory activation of Kupffer cells and MoMFs involves the Tool-like receptors TLR4 and TLR9 (Wen et al 2021) as well as the inflammasome responses. In this latter respect, the NLR family pyrin domain containing 3 (NLPR3) and absent in melanoma 2 (AIM2) inflammasomes have been shown to contribute to various liver diseases (Szabo and Csak 2016).

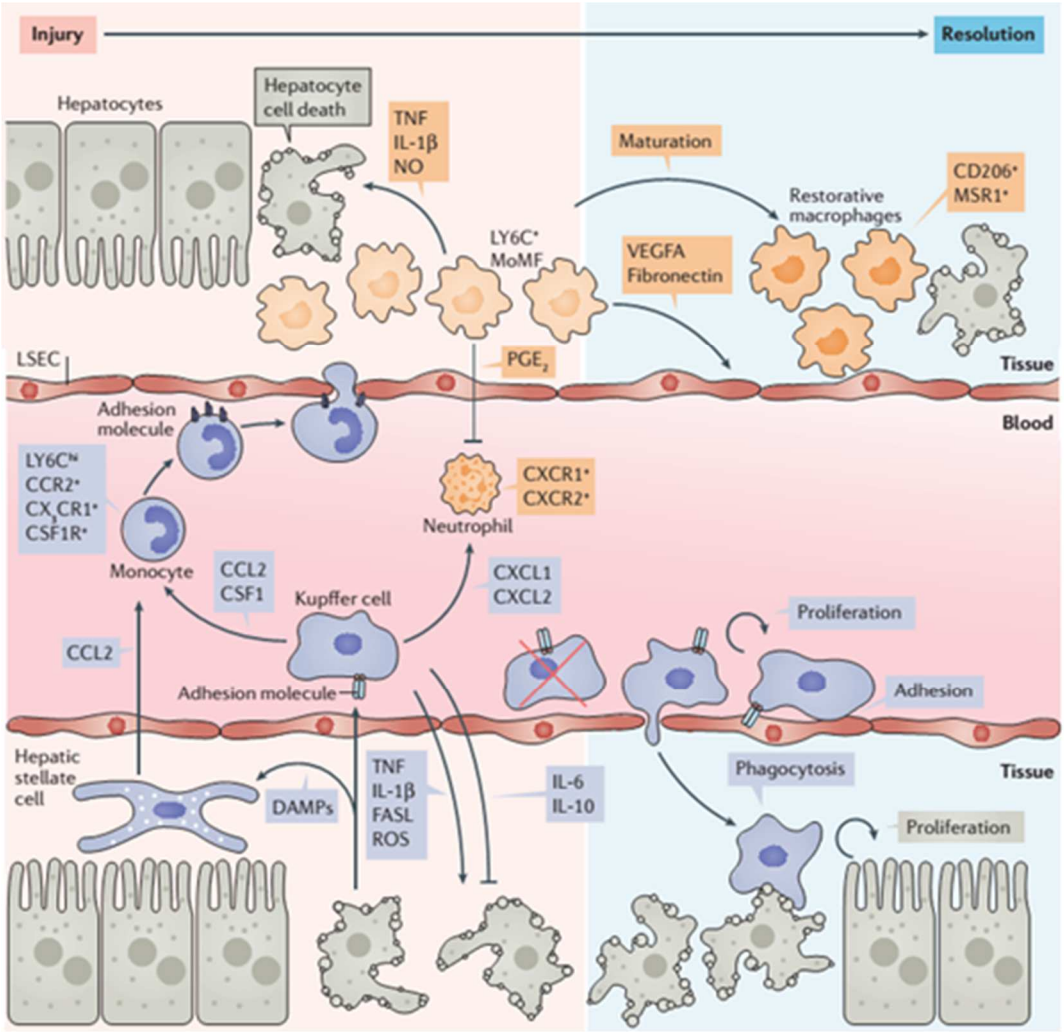

Introduction Figure II: Role of hepatic macrophages in acute liver damage (From Krenkel and Tacke 2017).

During the evolution of acute liver damage in response to CSF1, the Ly6C^{high} MoMFs around the areas of hepatic necrosis shift to Ly6C^{low} macrophages (Introduction Fig II; Krenkel and Tacke 2017). This change is characterized by the downregulation of CCR2 and the

upregulation of CX_3CR1 (Dal-Secco et al. 2015). Ly6c^{low} MOMFs produce anti-inflammatory mediators including IL-10, metallo-proteases (MMP9, MMP12, and MMP13), hepatocyte growth factor (HGF) and insulin-like growth factor (IGF), and express phagocytosis-related genes such as MARCO and c-met protooncogene tyrosine kinase (MerTK). These features make Ly6c^{low} MOMFs responsible for the termination of inflammation, the clearance of necrotic cells debris and apoptotic bodies as well as for the initiation of extracellular matrix repair and the restoration of sinusoidal vessels (Wen et al 2021) (Introduction Fig. II). This latter process involves MoMF interaction with sinusoid endothelial cells which promotes vessel sprouting through the release of vascular endothelial growth factor A (VEGF-A) and matrix metallopeptidase 9 (MMP9) (Ehling et al. 2014). Interestingly, mice defective in CCR2 and lacking infiltrating monocytes show a prolonged repair phase after acetaminophen-induced liver injury (Holt et al. 2008; Zigmond et al. 2014).

A further key aspect of liver repair following acute damage concerns the recovery of parenchymal cells mass due to the proliferation of mature hepatocyte and in some instance of hepatic progenitor cells (HPCs, also termed oval cells) (Michalopoulos and Bhushan 2021). Experiments using rodent models of partial hepatectomy have shown that both Kupffer cells and MoMFs play important roles in promoting hepatocyte proliferation since Kupffer cells depletion by mice treatment with by liposome-entrapped clodronate (CLDN) delays liver regeneration after partial hepatectomy by reducing the production of TNFα and IL-6 that are important for the initiation of hepatocyte proliferation (Wen et al. 2021). In fact, macrophage derived TNFα enhances the production of IL-6, which directly induces hepatocyte entry into the cell cycle through the activation of STAT3-mediated signals (Michalopoulos and Bhushan 2021). In a similar manner, following extensive hepatocyte loss, the proliferation of HPCs also requires macrophage-mediated stimuli (Wen et al. 2021). In this setting, MoMFs are the source of Wnt3a, that favours liver progenitor cell differentiation toward hepatocytes (Boulter et al. 2019).

The mechanisms that promote MoMF phenotype shifting during the repair from acute injury are still incompletely characterized. Efferocytosis of apoptotic cell bodies mainly derived from dying neutrophils appears a major mechanism involved in this switching. During this process the recognition of apoptotic bodies mediated by MerTK receptors along with IL-4 and IL-13 signalling drive the differentiation of MoMFs into an anti-inflammatory and tissue

reparative phenotype (Bosurgi et al. 2018; Triantafyllou et al. 2018). In fact, mice deficient in MerTK exhibit a reduced number of Ly6C^{low} MoMFs and impaired resolution of inflammation following acetaminophen poisoning (Triantafyllou et al. 2018). Beside efferocytosis, other stimuli can contribute to induce changes in macrophage phenotype. For instance, ROS produced by neutrophils have been shown to play this role through the activation of a Ca^{2+}-dependent AMP kinase (Yang et al. 2019). IL-4 produced by $CD4^+$ T-lymphocytes is a further mediator of macrophage differentiation since in mice infected with *Schistosoma mansoni*, $CD4^+$ T-cells depletion blocks the phenotypic switch of Ly6C^{high} MoMFs (Girgis et al. 2014). Recent studies have also outlined the importance of the triggering receptor expressed on myeloid cells 2 (TREM-2) in down-modulating inflammatory responses in liver MoMFs. TREM-2 is a membrane receptor widely distributed in myeloid cells that acts through the adapter molecule DAP12 in dampening cytokine responses and promoting the shifting to Ly6C^{low} phenotype (Coelho et al 2021). Accordingly, mice lacking TREM-2 show increased parenchymal damage and inflammation along with an impaired repair following acute liver damage (Perugorria et al. 2019; Coelho et al. 2021). Finally, during liver repair macrophage death also appears to play a role in modulating the shift from pro- to anti- inflammatory functions (Wen et al. 2021) and defects in the regulation of MoMF apoptosis by fork head box O3 (FOXO3)-dependent signals causes hyperinflammation and increased sensitivity to liver injury induced by mice treatment with ethanol and endotoxin (Li et al. 2018).

1.5) Liver macrophage in chronic liver diseases

Chronic liver disease caused by chronic hepatitis B (HBV) and C virus (HCV) infection, metabolic imbalances such as nonalcoholic steatohepatitis (NASH), alcohol abuse, biliary obstruction and iron overload are characterized by prolonged cycles of iterative bursts of tissue damage and inflammation which cause a progressive derangement of hepatic architecture due to hepatocyte loss, liver matrix and vascular network impairment and extensive deposition of scar collagen, ultimately leading to hepatic fibrosis and cirrhosis (Tsochatzis et al. 2014). At present, liver cirrhosis represents the main cause of liver failure and is the 14th most common cause of death worldwide as well as an important risk factor in the development of hepatocellular carcinoma (HCC) (Tsochatzis et al. 2014).

It is increasingly clear that in chronic liver diseases the progression to fibrosis/cirrhosis is fuelled by hepatic inflammation that accompany dysregulated wound healing with excessive deposition of extracellular matrix (ECM) (Weston et al. 2019). In this setting liver macrophages are essential for controlling both inflammatory and fibrogenetic responses, while hepatic macrophage depletion alleviates fibrogenesis in mice (Weston et al. 2019). Indeed, in the early stage of liver injury, Kupffer cells secrete CCL2 to recruit Ly6C^{high} MoMFs which exhibit a combined proinflammatory and profibrogenic phenotype characterized by secretion of TNFα, IL-1β, IL-6, CCL2 and CCL5 along that of cytokines and growth factors such as Tumour Growth Factor β (TGFβ), Platelet Derived Growth Factor (PDGF) and Connective Tissue Growth Factor (CTGF) which support the activation of hepatic stellated cells (HSCs) to matrix producing myofibroblasts (Introduction Fig III-Krenkel and Tacke 2017; Weston et al. 2019).

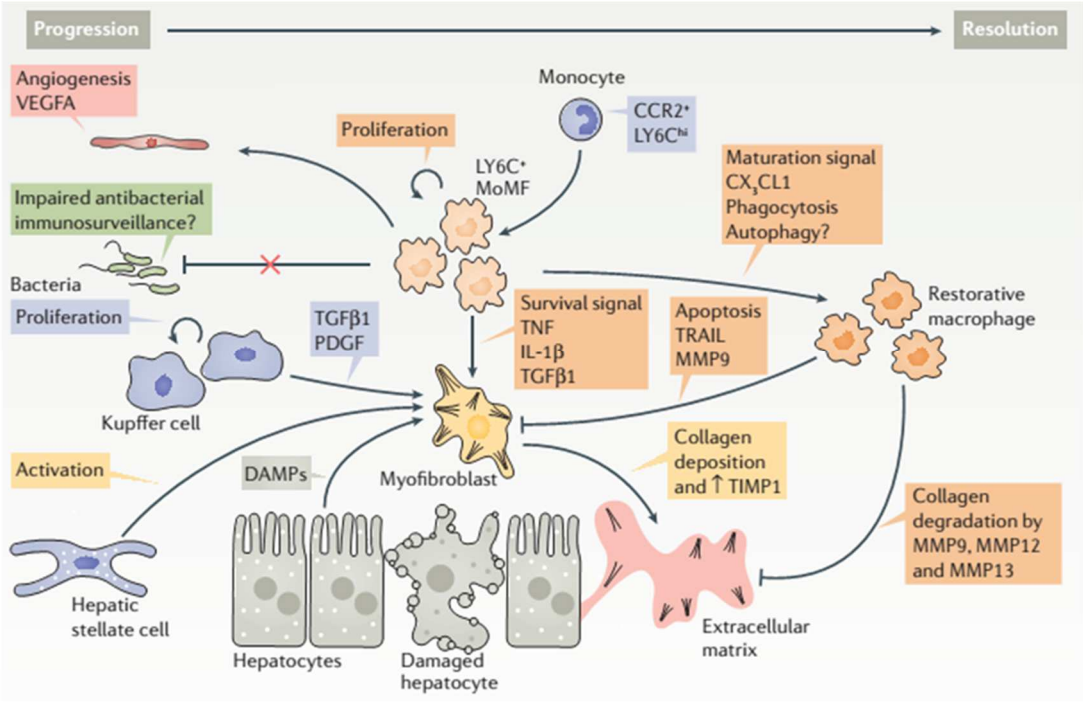

Introduction Figure III: Role of hepatic macrophages in the development of liver fibrosis (From Krenkel and Tacke 2017 Modified).

Nonetheless, also proinflammatory cytokines and chemokines (TNFα, IL-1β, IL-6 and CCL5) are important in the interaction with HSCs to establish a profibrogenic niche (Krenkel et al. 2018). In humans, such a capacity of activating HSCs appears to involve CD14^{+}/CD16^{+} MoMFs (Tacke and Zimmermann 2014).

Along this line it has been observed that interference with chemokine signalling by the CCR2/CCR5 receptor inhibitor cenicriviroc effectively blocks CCL2-mediated monocyte liver recruitment and to exert anti-inflammatory and antifibrotic effects in various mouse models of chronic liver injury (Kruger et al. 2018). Clinical trials have also shown that cenicriviroc is effective in improving the evolution of liver fibrosis in patients with NASH (Ratziu et al. 2020). Nonetheless the role of MoMFs in the evolution of chronic liver diseases appears more complex since Ly6C^{low} MoMFs also display an antifibrotic activity related to an enhanced expression of metalloprotease such MMP9, MMP12 and MMP13 that are effective in matrix degradation (Ramachandran et al. 2012). In fact, it has been observed that in experimental models of liver fibrosis the interference with the recruitment of Ly6C^{high} MoMFs enhances the Ly6C^{low} fraction and attenuates fibrogenesis leading to resolution of fibrosis (Baeck et al. 2014). In a similar manner, macrophage phagocytosis of injected liposomes induces the switch of Ly6C^{high} MoMFs to Ly6Cl^{ow} MoMFs and accelerates regression of liver fibrosis (Ramachandran et al. 2012). Ly6Cl^{ow} MoMFs have also the capability of reversing myofibroblast activation to quiescent HSCs or to induce their disappearance through apoptosis or cell senescence (Tacke and Trautwein et al. 2015).

So far little is known about the mechanisms that are implicated in promoting the combined proinflammatory and profibrogenic activity of MoMFs associated to chronic liver disease evolution. It is well possible that the continuous presence of DAMS released by damaged hepatocytes might contribute to sustain Ly6C^{high} MoMFs phenotype as well as to promote the continuous recruitment of new monocytes. Furthermore, in mouse models of liver fibrosis Ly6C^{high} MoMFs express CXCL16 which stimulates the liver migration of natural killer T (NKT) cells that, in turn, sustain proinflammatory and fibrogenetic responses (Wehr et al. 2013). In a similar manner the interaction with other immune cells such as T-lymphocytes (Sutti and Albano et al. 2020) or specific metabolic factors might also contribute to main Ly6C^{high} MoMF phenotype in different pathological conditions. On this latter respect, Ioannou and co-workers (Ioannou et al. 2013; 2015) have shown that in experimental NASH the accumulation of cholesterol crystals within liver macrophages drives their activation through the stimulation of NLPR3 inflammasome. Interestingly, enlarged macrophages with a foamy appearance due to the accumulation of cytoplasmic lipid droplets and cholesterol crystals are a feature of human NASH (Itoh et al. 2013) where they form aggregates reminiscent of crown-

like structures detectable in the adipose tissue of obese subjects (Shapiro et al., 2013). The characterization of these cells has shown that they are prevalently Ly6C^{high} and have a proinflammatory phenotype consistent with those of Ly6C^{high} MoMFs (Zigmond et al., 2014; Jindal et al 2015) but are also producing anti-inflammatory mediators such as IL-10 and annexin A1 (Jindal et al 2015). These observations suggest that a variety of stimuli within the liver environment might influence macrophage phenotype, thus favouring their heterogeneity and the different contribution to the evolution of liver diseases.

Adding complexity to this scenario recent studies using single-cell RNA sequencing of liver macrophages has revealed that MoMFs expanding in either human and rodent NASH, have a specific phenotype, characterized by the expression of the Triggering Receptor Expressed on Myeloid cells 2 (TREM-2), CD63 and the glycoproteins CD9 and NMB (GPNMB). The prevalence of these cells, named NASH-associated macrophages (NAM), in human NASH correlates with the severity of steatohepatitis and fibrosis (Xiong et al. 2019), likely in relation to their capability of producing pro-fibrogenic mediators such as osteopontin (OPN) and galectin-3 (Gal-3) (Xiong et al. 2019; Seidman et al 2020; Remmerie et al. 2020). Furthermore, NAMs appear to be the main components of crown-like macrophage aggregates (Remmerie et al. 2020). Interestingly, Ramachandran and co-workers (Ramachandran et al. 2019) have recently demonstrated that the TREM-2/CD9/OPN/Gal-3 signature also characterizes CD68^{+}/MARCO^{-} scar-associated macrophages identified in human fibrotic livers. Lineage tracking indicates that NAMs and scar-associated macrophages derive from liver infiltrating monocytes (Jaitin et al. 2019; Remmerie et al. 2020) and acquire their phenotype in response to specific signals in interstitial liver niche (Sakai et al. 2019; Xiong et al. 2019). These latter observations open the possibility that specific cell interactions might contribute to modulate macrophage plasticity during the evolution of liver damage adding new perspective in understanding the function of these cells.

2. Aim of the Project

In the recent years and increasing number of studies have investigated the mechanisms that modulates the functions of liver macrophages during the evolution of acute and chronic liver damage in the attempt of characterizing the signals that contribute to modulate the great functional plasticity of these cells in the switching from pro-inflammatory to repair functions as well as in promoting the liver disease progression to fibrosis/cirrhosis. Nonetheless, several issues remain poorly understood.

In my doctoral project, I have investigated some of these aspects focalizing my work on:

c) The role of the lymphocyte co-stimulatory molecule Inducible T-cell Costimulator (ICOS) in modulating macrophage functions during liver repair.

d) The capacity of the anti-inflammatory mediator Annexin A1 of influencing the pro-fibrogenic action of macrophages during the evolution of experimental nonalcoholic steatohepatitis (NASH)

These issues were addressed using a well-established experimental model of acute liver damage based on mice poisoning with the hepatotoxic agent carbon tetrachloride (Karlmark et al. 2009) and with a chronic model of liver damage reproducing the features human nonalcoholic steatohepatitis (NASH) obtained by feeding mice with methionine/choline deficient (MCD) diet or a high fat/carbohydrate diet which allows to reproduce the evolution of chronic liver inflammation to hepatic fibrosis (Lau et al.2017).

3. Materials & Methods

3.1 Mice acute liver injury.

Acute liver injury was induced by injecting intra-peritoneally mice with CCl_4 (0.6 ml/kg in olive oil). Control animals received an injection with olive oil alone. All animals were euthanized 24-72 hours after CCl_4 administration. In these experiments we used eight-week-old male wild-type C57BL/6, ICOS deficient (*ICOS*$^{-/-}$; strain B6.129P2-Icos^{tm1Mak}/J) and ICOSL deficient (*ICOS-L*$^{-/-}$; B6.129P2-Icosl^{tm1Mak}/J) mice in C57BL/6 background obtained from The Jackson Laboratories (Bar Harbor, Maine, USA). In some experiments mice were treated with murine recombinant ICOS bound to the human IgG1 Fc portion (ICOS-Fc) . ICOS-Fc (100 µg in sterile saline) was administered to mice by intraperitoneal injection 24 hours after CCl_4 and then every 12 hours up to 48 hours. Control animals received a similar amount of saline alone.

Hepatic $CD8^+$ T cells ablation was obtained by injecting WT mice with rat IgG2b anti-mouse CD8β monoclonal antibody (clone YTS 156.7.7). The animals received YTS 156.7.7 mAb (100 µg) three days before and immediately after CCl_4 challenge. Control animals received the same amount of isotype matched IgGs. YTS 156.7.7 anti-CD8β monoclonal antibody was a kind gift by Dr. Stephen Cobbold, William Dunn School of Pathology, University of Oxford, (Oxford, UK).

The animal experiments comply with ethical guidelines for animal experimentation. The protocols were approved by the Italian Ministry of Health (authorization No. 84/2021-PR) according to the European legal requirements.

3.2 Induction of chronic liver damage and fibrosis in mice

Steatohepatitis was induced by feeding eight-week-old male wild type C57BL/6 mice with either a methionine/choline deficient (MCD) diet for 2 or 8 weeks or with a high fat/carbohydrate diet enriched with 1.25% cholesterol Western Diet (WD) for 10-16 weeks (Laboratorio Dottori Piccioni, Gessate, Italy). Control animals received a diet supplemented by either choline/methionine or standard chow diet. Mice were treated for 5 days a week by daily intraperitoneal injection of human recombinant AnxA1 (hrAnxA1; 1 µg/daily in saline) according to a previously published protocol that allowed effective pharmacokinetic and avoided production of neutralising antibodies. Control animals received an injection of saline

alone. At the end of the treatments, mice were anaesthetized with sevoflurane, and after checking the anesthesia depth, the blood was collected by retro-orbital bleeding. Afterwards, the mice were euthanized by cervical dislocation. Animal experiments were performed at the animal facility of the Dept of Health Sciences, University of East Piedmont (Novara, Italy) and comply with EU ethical guidelines for animal experimentation. The study protocols received ethical approval by the Italian Ministry of Health (authorization No. 449/2019-PR) according to the European law requirements.

***3.3 AnxA1 Recombinant Protein Purification*.**

cDNA of hrAnxA1 carrying a cleavable N-terminal poly-His tag was expressed in Escherichia coli and purified as previously reported (Karlmark et al; 2010). The purity of recombinant AnxA1, was assessed by sodium dodecyl sulphate-polyacrylamide gel electrophoresis and matrix-assisted laser desorption/ionization dual time-of-flight mass spectrometry and was >95%.

***3.4 Assessment of liver injury*.**

Livers were rapidly removed, rinsed in ice-cold saline, and cut into five pieces. Aliquots were immediately frozen in liquid nitrogen and kept at −80°C until analysis. Two portions of the left lobe from each liver were fixed in 10% formalin for 24h and embedded in paraffin. 4 µm tick liver sections were stained with hematoxylin/eosin using a Roche Ventana HE 600 automatic staining system (Roche Diagnostics International AG, Rotkreuz, Switzerland), while collagen deposition was detected by Picro-Sirius Red staining. Sections were scored blindly for steatosis and lobular inflammation and the extension of fibrosis as described (Giulliams et al; 2016). Microphotographs were taken using a Nikon Eclips CI microscope fitted with a DSR12 camera (Nikon Europe BV, Amsterdam, Netherlands) using the NIS-Elements F4.60.00 acquisition software. The extension of necrotic areas and of fibrosis was assessed by histo-morphometric analysis in, respectively, hematoxylin/eosin-stained liver sections using the ImageJ 1.53e software (National Institute of Health, Bethesda, MD, USA.

Plasma ALT levels and liver triglycerides were determined by spectrometric kits supplied, respectively, by Gesan Production SRL (Campobello di Mazara, Italy) and Sigma Aldrich (Milano, Italy).

3.5 Histology and immunohistochemistry.

To detect liver macrophages, tissue sections were stained in formalin-fixed sections using rabbit polyclonal antibodies against F4-80 and goat polyclonal antibodies against galectin-3 provided by, respectively, Abcam (Cambridge, UK) and R&D Systems (Minneapolis, USA) in combination with a horseradish peroxidase polymer kit (Biocare Medical, Concord, CA, USA).

The immunostaining for the proliferation marker Ki67 and ICOSL was performed in paraffin fixed section using anti-Ki67 monoclonal antibody (clone 30-9) and anti-ICOSL goat polyclonal antibodies (CD275 cod PA5-47161) (Thermo Fisher Scientific, Milano, Italy) in an automated staining system (BenchMark ULTRA IHC/ISH System, Roche Diagnostics International AG, Rotkreuz, Switzerland). In some experiments the staining with anti-ICOSL antibodies was also evidenced in frozen liver sections by immunofluorescence using Alexafluor®-546 donkey anti-goat IgG (H+L) (Thermo Fisher Scientific, Milano, Italy) and Leica DM 5500B fluorescence microscope and Leica Application Suite X (Leica Microsystems (Buccinasco, Italy). Plasma ALT levels were determined by a spectrometric kit supplied by Gesan Production SRL (Campobello di Mazara, Italy).

3.6 Flow cytometry analysis of liver leukocytes.

Livers were digested by type IV collagenase from Clostridium histolyticum (Sigma-Aldrich, St. Louis, MO, USA), and intrahepatic leukocytes were isolated by multiple differential centrifugation steps according to (Karlmark K.R et al;2010). The cell preparations were then subjected to red cell lysis by RBC Lysis Buffer (eBioscience, Thermo Fisher Scientific, Milano, Italy) and stained using combinations of the following monoclonal antibodies: CD45 (Clone 30-F11, Cat. 12-0451-82), CD3 (Clone 17A2, Cat. 17-0032-82) CD4 (Clone GK1.5, Cat. N. 56-0041-80) CD8 (Clone 53-6.7, Cat. 11-0081-82), Ly6C (Clone HK1.4, Cat. 53-59-32-80), NK1.1 (Clone PK136, Cat. 12-5941-81), Ly6G (Clone RB6-8C5, Cat. 47-5931-82), MHCII (Clone M5/114.15.2, Cat. 56-5321-80), CD103 (Clone 2E7, Cat. 12-1031-81), CD69 (Clone H1.2F3, Cat. 12-0691-82), CD107a (Clone eBio1D4B, Cat. N. 12-1071-81), CD206 (Clone MR6F3, Cat. 25-2061-80) MerTK (Clone DS5MMER, Cat. N. 56-5751-80 eBioscience, Thermo Fisher Scientific, Milano, Italy), CD11b (Clone M1/70, Cat. 101212), ICOS (Clone 15F9, Cat. 107705), ICOSL (Clone HK5.3, Cat. 107405), F4-80 (Clone BM8, Cat. 123113, Biolegend, San Diego, CA, USA), TREM-2 (Clone 78.18, Cat. MA5-28223, Thermo Fisher Scientific, Milano, Italy). In some

experiments, macrophage viability was evaluated by cell staining using the rh-annexin V/FITC kit (Bender Med Systems, Vienna, Austria). Sample analysis was performed using the Attune NxT flow-cytometer (Thermo Fischer Scientific, Waltham, MA, USA) and data were elaborated with FlowJo™ Software (BD Biosciences, San Jose, CA, USA).

3.7 mRNA extraction and Real-time PCR.

mRNA was extracted from snap-frozen liver fragments using the TRIzol® Reagent (Thermo Fischer Scientific, Milano, Italy) as previously reported [20]. cDNA was generated from 1 µg of mRNA using the High-Capacity cDNA Reverse Transcription Kit (Applied Biosystems Italia, Monza, Italy) in a Techne TC-312 thermocycler (TecneInc, Burlington NJ, USA). Real-Time PCR was performed in a CFX96™ Real-time PCR System (Bio-Rad, Hercules, California, USA) using TaqMan Gene Expression Master Mix and TaqMan Gene Expression probes for mouse TNF-α (Mm99999068_m1), CCL2 (Mm00441242_m1), CD11b (Mm00434455_m1), TREM-1 (Mm01278455_m1), CD206 (Mm01329362_m1), TREM-2 (Mm04209422_m1), MerTK (Mm00434920_m1), CX_3CR1 (Mm00438354_m1) and beta-actin (Cat. N 4352663, Applied Biosystems Italia, Monza, Italy). All samples were run in duplicate, and the relative gene expression was calculated as $2^{-\Delta Ct}$ over that of β-actin gene.

3.8 Metabolic assessment.

After overnight fasting mice receiving the high fat/carbohydrate diet Western Diet (WD) or standard diet for 16 weeks received a single intraperitoneal injection of D-glucose (1,5 g/kg body weight). Blood sampling was performed by tail vein incision with sterile needles and glycaemia was measured by a glucometer (Menarini Diagnostics, Milan, Italy) before and after 10, 30, 60, 90, and 120 minutes from glucose administration.

3.9 Data analysis and statistical calculations.

Statistical analyses were performed by SPSS statistical software (SPSS Inc. Chicago IL, USA) using one-way ANOVA test with Tukey's correction for multiple comparisons or Kruskal-Wallis test for non-parametric values. Significance was taken at the 5% level. Normality distribution was assessed by the Kolmogorov-Smirnov algorithm.

4. Results Section 1

Inducible T-cell Costimulator (ICOS) mediates lymphocyte/macrophage interactions during liver repair

Data published on Front Immunol. 2021; 12:786680. doi: 10.3389/fimmu.2021.786680.

4.1 Foreword

Acute liver injury resulting from viral infections, ischemia/reperfusion or adverse drug responses is the main factor in the pathogenesis of acute liver failure (ALF), a syndrome characterized by high mortality in the absence of immediate intensive care and/or emergency liver transplantation (Bernal W et al.2013; Montrief T et al.2019). It is increasingly clear that beside hepatocyte damage inflammatory reactions play an important role in the pathogenesis of acute liver injury and are critical in the processes of parenchymal regeneration (Mc Donald B et al.2016; Jaeschke H et al 2020). Animal studies have shown that inflammatory responses triggered by hepatocyte damage largely depend upon the massive recruitment and activation of granulocytes and monocytes-derived macrophages (MoMFs), which, on their turn, contribute to tissue damage by releasing pro-inflammatory mediators, reactive oxygen species (ROS), nitrogen monoxide (NO) and granule enzymes. (Mc Donald B et al.2016; Jaeschke H et al 2020). Nonetheless, upon cessation of parenchymal damage MoMFs undergo functional changes characterized by the downregulation of the pro-inflammatory activity and the stimulation in the capability of scavenging death cells and of promoting tissue repair (You Q et al.2013; Cho Y et al. 2021). As mentioned in the introduction this phenotype switch associates with the down modulation of the monocyte marker lymphocyte antigen 6 (Ly6C), also known as tissue plasminogen activator receptor, and of CCL2 chemokine receptor CCR2 with the concomitant increase in the expression of fractalkine receptor (CX_3CR1) (Zigmond E et al. 2014; Dal Secco D et al. 2015) as well as of the mannose receptor (CD206) and the efferocytosis receptor c-Met Proto-Oncogene Tyrosine Kinase (MerTK) (Wen Y et al.2021). Several factors including the cytokine milieu and the efferocytosis of apoptotic bodies are involved in promoting MoMF switching to a pro-repair phenotype (Wen Y et al.2021). However, it is likely that additional cell-mediated signals might be also involved in modulating

MoMF functions, since it is now evident that direct intracellular interactions in liver niche environment are critical for MoMF differentiation to Kupffer cells (Sakai M, Trautman TD et al. 2019).

Previous studies have shown that lymphocyte interaction with myeloid cells mediated by Inducible T-cell costimulator (ICOS; CD278) and its ligand (ICOSL; CD275, also named B7h, B7-H2) potentiates lymphocyte IL-4 production [13] and contributes to skin wound healing in mice (Maeda S et al. 2011). ICOS belongs to the CD28 family of co-stimulatory molecules, and it is selectively expressed by activated $CD4^+$ and $CD8^+$ T-cells together with other co-stimulatory molecules of the same family (Wikenheiser D.J et al. 2016). Conversely, ICOSL is constitutively present on the surface of a variety of myeloid cells including dendritic cells, macrophages, B-cells but also on endothelial cells, lung epithelial cells and fibroblasts (Wikenheiser DJ et al. 2016). The triggering of ICOS on T-cells by ICOSL has been shown to modulate lymphocyte cytokine secretion pattern and, in some conditions, to favour regulatory T-cell (Treg) differentiation (Li DY et al.2020). In addition, ICOS/ICOSL interaction plays an important role in the development and differentiation of Follicular T-helper cells (Tfh) in the germinal centres of lymphatic nodes (Wikenheiser DJ et al. 2016). However, recent reports have shown that ICOS/ICOSL interaction can also trigger reverse signals able to modulate the functions of ICOSL-expressing cells. For instance, ICOSL-mediated signals favour dendritic cells maturation stimulating cytokine secretion and antigen presentation (Tang G et al.2009; Occhipinti et al. 2013). while they prevent monocytes differentiation to osteoclasts (Gigliotti CL et.2016).

From this background, and the the report by Maeda and colleagues of a dramatic delay in skin wound healing in both *ICOS*$^{-/-}$ and *ICOSL*$^{-/-}$ mice (Maeda S et al. 2011), we have investigated the contribution of ICOS/ICOSL dyad in modulating lymphocytes/MoMFs interactions in the evolution of acute liver damage.

4.2 Experimental data

a.) ICOS is up regulated in T-lymphocytes in response to acute hepatic injury.

According to previous studies (Karlmark K.R et al. 2010; Sutti S et al. 2017), acute liver injury caused by mice poisoning with the hepatotoxic agent carbon tetrachloride (CCl_4) leads to centrilobular necrosis and an extensive inflammatory response which peaked after about 24 hours and rapidly declined thereafter with an almost complete recovery after 72 hours (Fig. 1A). Besides liver infiltration by phagocytes, hepatic inflammation also involved the recruitment of both $CD4^+$ helper and $CD8^+$ cytotoxic T-lymphocytes (Fig. 1C). Flow cytometry analysis showed that liver infiltrating T-lymphocytes expressed ICOS and that the overall prevalence of $CD3^+/ICOS^+$ cells followed the evolution of the inflammatory process, being maximal around 24 hours (Fig 2A) and declining in the recovery phase, mainly in relation to the lowering in $CD4^+$ T-cell prevalence (Fig. 2B). However, liver healing did not affect the prevalence of ICOS-positive $CD8^+$ T-cells infiltrating the liver after 72 hours, which instead further increased as compared to early time points (Fig. 2B). These $CD8^+$ T lymphocytes comprised both $CD103^+$ and $CD103^-$ cells and expressed the activation markers CD69 and CD107a (Fig. 3). In the same animals, we also observed an early up regulation in the hepatic expression of ICOSL, which mainly involved $CD11b^{high}$/F4-80^+ MoMFs, (Fig. 2C). The fraction of ICOSL-positive MoMFs was well appreciable at the peak of inflammation and further increased during the recovery phase (Fig. 2C). Consistently, immunostaining with an anti-ICOSL polyclonal serum of liver sections from CCl_4-treated at 72 hours showed selective labelling of infiltrating MoMFs in centrilobular areas, while no staining was appreciable in control livers (Fig. 4).

b.) ICOS signaling did not affect the evolution of inflammatory responses associated to acute liver injury.

From these data, we investigated whether interfering with ICOS/ICOSL signalling might affect the evolution of damage-associated hepatic inflammation. Time course analysis of the liver transcripts for pro-inflammatory markers in wild-type (WT) and ICOS knockout (*$ICOS^{-/-}$*) mice receiving CCl_4 showed the same pattern in the up-regulation and decline of tumor necrosis factor-α (TNF-α), CCL2 and the leukocyte integrin αM (CD11b) mRNAs, even though the down-modulation of these markers was more rapid in *$ICOS^{-/-}$* mice (Fig.5) In line with these findings,

also the expression of the Triggering Receptor Expressed on Myeloid cells 1 (TREM-1), a membrane receptor involved in regulating the pro-inflammatory activity of neutrophils and macrophages (Arts RJ et al. 2013), was comparable in the two strains. Consistently, flow cytometry analysis of liver MoMFs did not evidence appreciable difference in the hepatic recruitment of Ly6C^{high}/CD11b^{high}/F4-80^{+} pro-inflammatory MoMFs between WT and *ICOS*$^{-/-}$ mice 24 hours after CCl_4 administration (Fig. 6A). ICOS absence also did not affect the functional maturation of MoMFs with the expression of high levels of Class II Mayor Histocompatibility Complex (MHCII) (Fig 6A) as well as the up regulation of the fractalkine receptor CX_3CR1 (Fig. 6B) (Dal Secco D et al.2015; S et al. 2017).

c.) ICOS deficiency interferes with liver healing following acute CCl_4 poisoning.

In line with the pattern of liver inflammation, we observed that after 24 hours from CCl_4 challenge, the extent of hepatic injury was similar in WT and *ICOS*$^{-/-}$ mice, despite circulating alanine aminotransferase (ALT) was slightly higher in these latter (Fig. 7A). However, while in WT mice hepatic circulating ALT appreciably declined after 48 hours from CCl_4 poisoning and liver damage almost completely recovered within 72 hours, ALT elevation persisted in *ICOS*$^{-/-}$ mice at 48 hours (Fig. 7A). Liver histology confirmed that *ICOS*$^{-/-}$ mice failed to clear centrilobular necrosis during the recovery from CCl_4 intoxication (Fig. 7C). Furthermore, 5 out 13 (38%) of CCl_4-treated *ICOS*$^{-/-}$ mice died by acute liver failure between 48 and 72 hours (Fig. 8A). At 72 hours the *ICOS*$^{-/-}$ mice who survived showed serum ALT about two folds higher than WT animals and still evident centrilobular necrotic areas (Fig. 7A-C). In these animals, the immunostaining for the proliferation marker Ki67 did not evidence significant differences in the labelling of hepatocyte nuclei as compared to the wild-type littermates (Fig. 8B), suggesting that interfering with ICOS/ICOSL signaling does not affect hepatocyte regeneration but it might affect the responses of non-parenchymal cells.

d.) ICOS signaling is required for the reparative response of liver macrophages.

From the observation that the absence of ICOS affected the recovery from acute hepatic injury, we investigated whether this might involve the switching of MoMF phenotype occurring during the healing response. The analysis of the transcripts for markers of

reparative MoMFs such as the mannose receptor (CD206) and the efferocytosis receptor c-Met Proto-Oncogene Tyrosine Kinase (MerTK) (Cho Y et al. 2021), evidenced that the expression of both markers was dramatically reduced during acute inflammation and recovered to control values during liver repair (Fig. 9). Similarly, hepatic healing was associated with the up-regulation in the Triggering Receptor Expressed on Myeloid cells 2 (TREM-2) (Fig. 9), a plasma membrane receptor involved in the damping MoMF inflammatory response (Coelho I et al. 2021; Triantafyllou E et al. 2018). In these settings, *ICOS*$^{-/-}$ mice were less efficient than WT animals in up-regulating CD206, MerTK and TREM-2 (Fig. 9). Furthermore, by evaluating by flow cytometry the distribution of CD11b^{+}/F4-80^{+} MoMFs 72 hours after CCl_4 poisoning, we observed that the prevalence of MoMFs was lowered by about 30% in the livers of *ICOS*$^{-/-}$ mice (Fig. 10A) and that such a loss involved the fraction of CD206/TREM-2/MerTK positive reparative MoMFs (Fig. 10B). Along with the reduction in reparative MoMFs and the impaired clearance of necrotic areas, CCl_4 challenged *ICOS*$^{-/-}$ mice also showed the persistence of a sustained hepatic infiltration by Ly6G^{high}/CD11b^{+}/F4-80^{-} granulocytes (3.2 ± 0.7 % vs 8.6 ± 2.5 % of CD45^{+} cells; $p<0.01$), while the prevalence of other myeloid cells was not affected.

e.) ICOS expressing CD8^{+} T cells contribute to liver healing.

As mentioned above, during the recovery from CCl_4-induced hepatocyte injury, ICOS was prevalently expressed by liver CD8^{+} T cells, while ICOSL was up regulated in MoMFs. To explore the possibility that the interaction between CD8^{+}/ICOS^{+} T cells and ICOS-L^{+} MoMFs might contribute to liver healing, we depleted liver CD8^{+} T cells using an anti-CD8 monoclonal antibody (mAb). Figure 11A shows that mice treatment with anti-CD8 mAb selectively lowered circulating and hepatic CD8^{+} T-cells. Furthermore, the overall prevalence of ICOS expressing CD3^{+} T cells within the liver was halved in the same animals 48 hours after CCl_4 (3.8 ± 0.4% vs 2.2 ± 0.6% of CD45^{+} cells; $p<0.02$). CD8^{+} T-cell depletion also specifically reduced the fraction of CD11b^{interm}/F4-80^{+}/CD206^{high} cells that were TREM-2 and MerTK positive without affecting that of CD11b^{high}/F4-80^{+}/CD206^{low} MoMFs (Fig. 11B). Such an effect was associated with a persistence of elevated ALT release and histological evidence of a delayed liver healing in CD8^{+} T cell-depleted mice 48 hours after CCl_4 challenge (Fig. 11C).

f.) ICOS-mediated signaling is required for the survival of liver reparative macrophages.

From the above results and the observation that CD206^{+}/TREM-2^{+}/MerTK^{+} MoMFs expressed ICOSL (Supplementary Fig. 12), we postulated that the reverse signaling triggered by the interaction of ICOS expressing CD8^{+} T-cells with ICOSL present in macrophages might influence the survival of reparative MoMFs. By labelling apoptotic cells with FITC-annexin V, we observed that the prevalence of annexin V-positive MoMFs in CCl_4-poisoned *ICOS*$^{-/-}$ mice was more than two folds higher than in similarly treated wild-type littermates (Fig. 13A). Interestingly, the treatment of *ICOS*$^{-/-}$ mice with murine recombinant ICOS bound to the human IgG Fc portion (ICOS-Fc) injected 24 hours after CCl_4 completely prevented the loss of hepatic MoMFs and rescued them from apoptosis (Fig. 13A). In particular, ICOS-Fc supplementation stimulated CD206 and MerTK transcripts and maintained the fraction of CD206^{+}/TREM-2^{+}/MerTK^{+} MoMFs (Fig. 13B). The possible role of ICOSL-mediated reverse signaling in regulating the survival of reparative MoMFs was further supported by the observation that mice deficient for ICOSL (*ICOSL*$^{-/-}$) showed a marked loss of MoMFs 72 hours after CCl_4 poisoning (Fig. 14A), which associated with an extensive annexin V staining (Fig. 14B) and an impaired recovery from acute hepatic damage (Fig. 14C).

g.) Recombinant ICOS improves acute liver damage in ICOS-deficient mice.

The observation that ICOS/ICOSL dyad was required for the survival of reparative liver MoMFs prompted us to evaluate the effects of ICOS-Fc on the evolution of CCl_4-induced acute liver damage in *ICOS*$^{-/-}$ mice. Using the same protocol of ICOS-Fc administration effective in preventing MoMF apoptosis, we observed a significant improvement of ALT release and a reduction in the extension of necrotic areas 48 hours after CCl_4 (Fig. 15A). All *ICOS*$^{-/-}$ animals receiving ICOS-Fc (6 out of 6) survived CCl_4 poisoning and histological evaluation revealed an almost complete recovery of liver necrosis after 72 hours (Fig. 15B). Consistently, at this time point circulating ALT levels in *ICOS*$^{-/-}$ mice receiving ICOS-Fc were lower than in *ICOS*$^{-/-}$ mice receiving saline and comparable with those in WT mice (Fig. 15B), supporting the hypothesis that ICOS-mediated signals are required for a full reparative response of liver infiltrating macrophages.

4.3) Figures Section 1

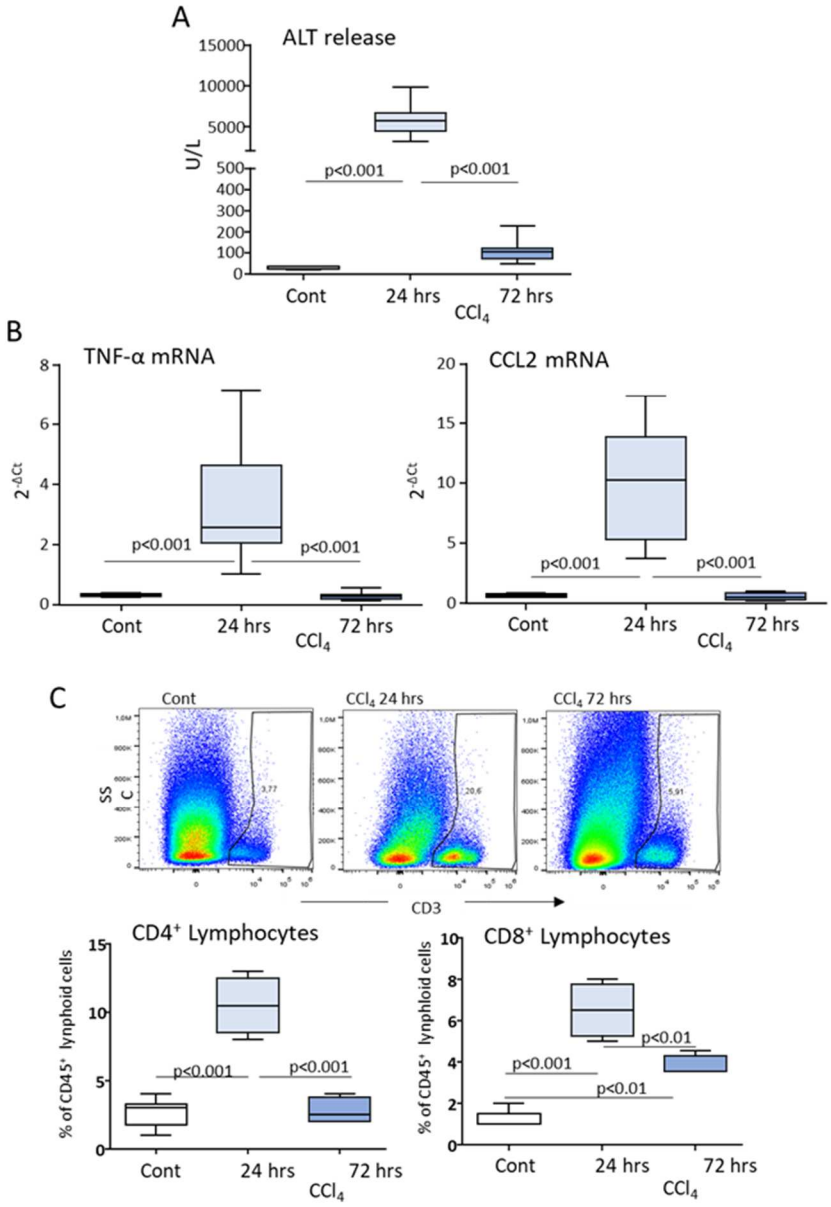

Figure 1: Hepatic lobular inflammation following acute liver injury promotes the liver recruitment of lymphocytes.

Parenchymal damage, lobular inflammation, and lymphocyte distribution in response to acute liver injury was analyzed in wild-type mice 24 and 72 hours after receiving an acute dose of CCl_4. Circulating levels of alanine aminotransferase (ALT) (Panel A). Real-Time PCR analysis of the hepatic expression of the macrophage inflammatory markers TNF-α and CCL2 (Panel B). Flow cytometry analysis of the liver distribution of $CD45^+/CD3^+/CD4^+$ helper and $CD45^+/CD3^+/CD8^+$ cytotoxic T cells, (Panel C). The values are expressed as mean ± SD of 5-6 animals.

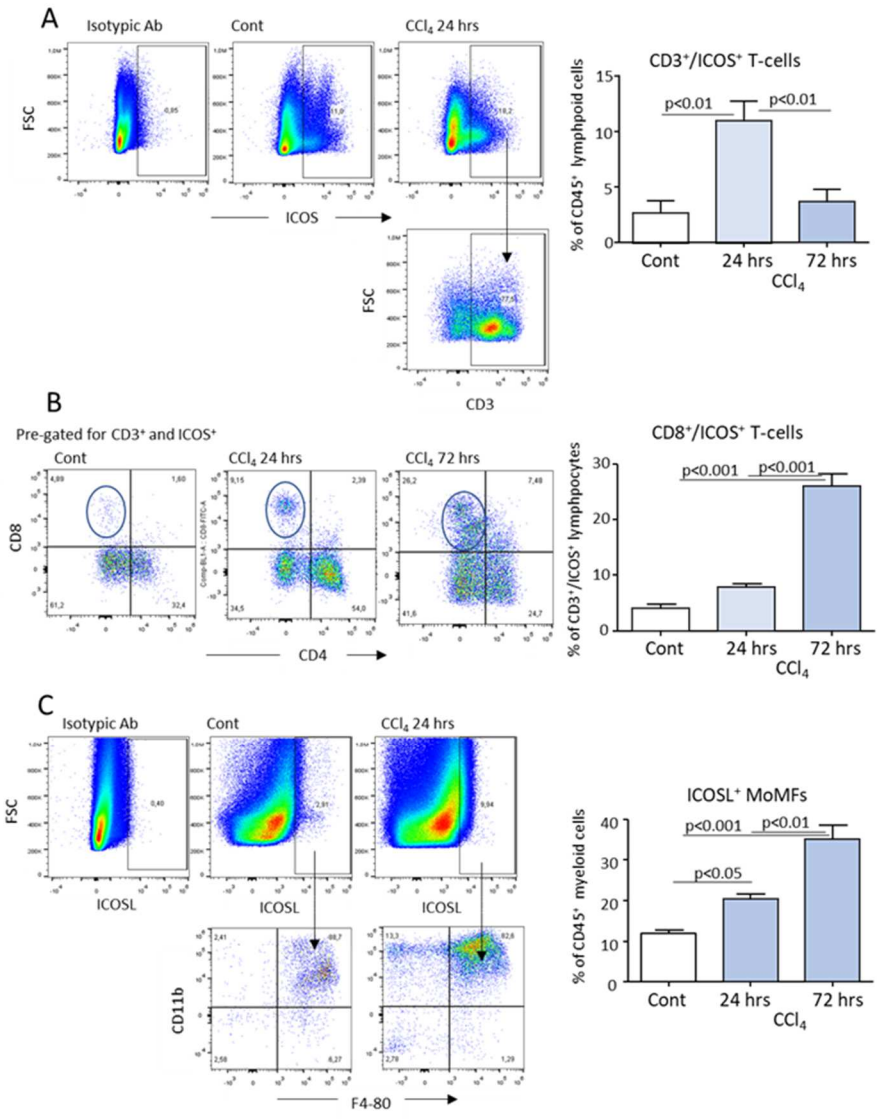

Figure 2: Expression of ICOS and ICOSL by lymphocytes and monocyte-derived macrophages (MoMFs) infiltrating the liver during acute inflammation.

Liver inflammation was induced in response to acute hepatocyte injury caused by carbon tetrachloride (CCl_4) in wild-type mice. The expression of ICOS was evaluated by flow cytometry in $CD3^+$ T-lymphocytes infiltrating the liver of control (Cont) and CCl_4-treated mice following 24 or 72 hours after challenge with the toxic agent (Panel A). Characterization of ICOS-expressing $CD3^+/CD4^+$ helper and $CD3^+/CD8^+$ cytotoxic T-cells in the liver of mice receiving CCl_4 for 72 hours (Panel B). Flow cytometry analysis of ICOSL expression among $CD11b^+/F4\text{-}80^+$ MoMFs (Panel C). The values are expressed as mean ± SD of 3-4 different cell preparations.

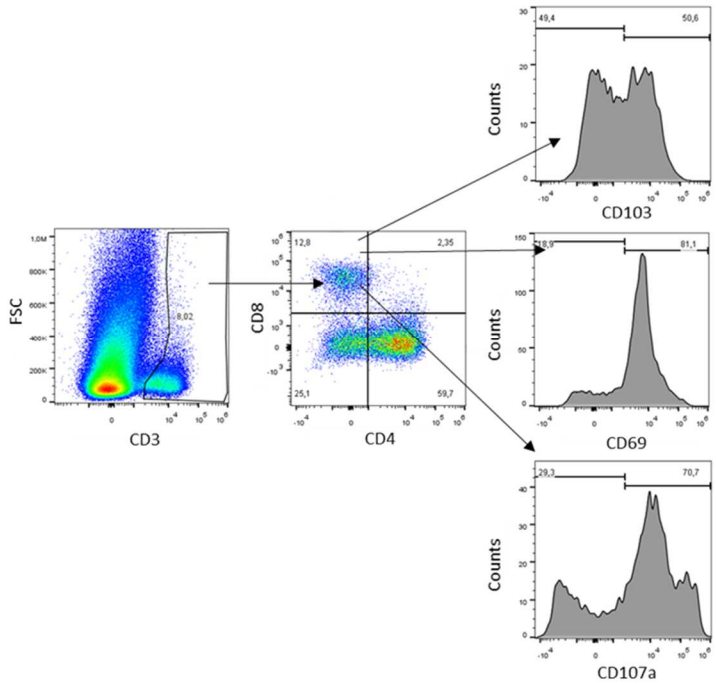

Figure 3: **Phenotypic characterization of ICOS expressing CD8⁺ T-lymphocytes.**

The expression of CD103 and of the activation markers CD69 and CD107a was evaluated by flow cytometry in $CD3^+/CD8^+$ cytotoxic T-cells obtained from the livers of mice receiving CCl_4 for 72 hours.

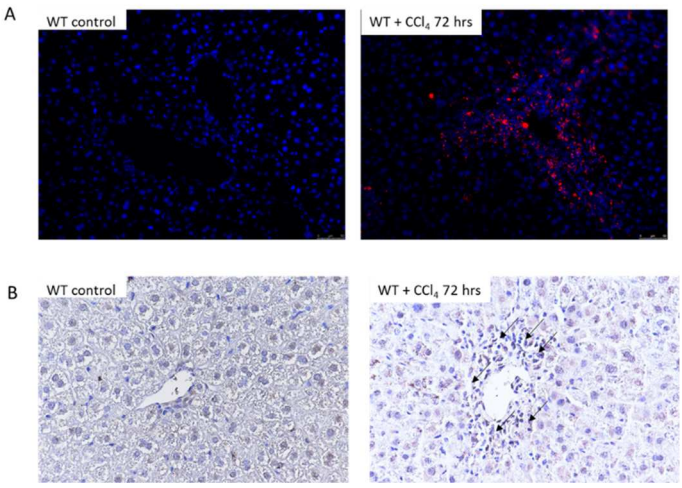

Figure 4: ICOSL is specifically expressed by liver infiltrating MoMFs.

Wild-type mice received or not CCl_4 for 72 hours. MoMF staining with an anti-ICOSL polyclonal goat antibody was evidenced by immunofluorescence (Panel A) in frozen liver sections using an Alexafluor®-labelled secondary antibody and confirmed by immunohistochemistry (Panel B) in paraffin fixed liver sections. Magnification 40X.

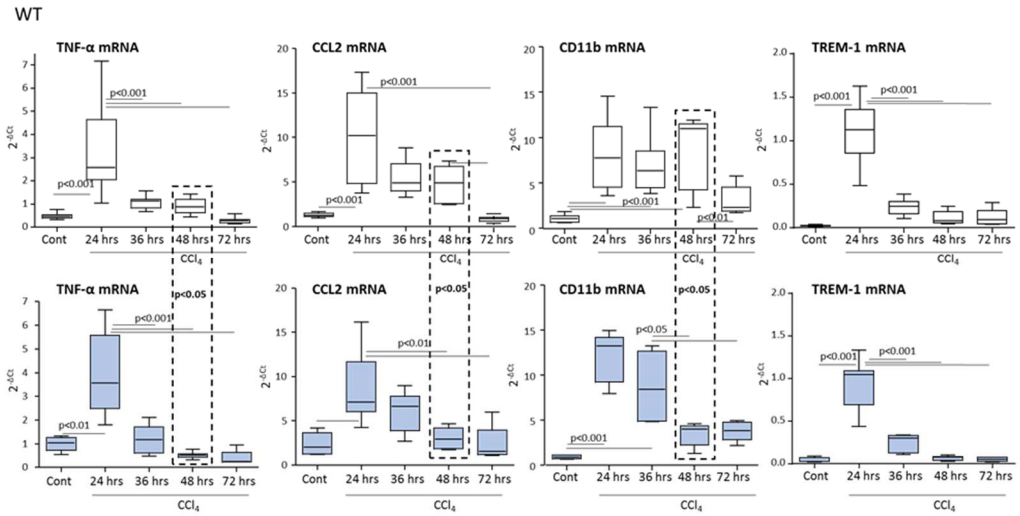

Figure 5: ICOS deficiency does not interfere with the evolution of hepatic inflammation associated to acute liver injury.

The transcripts of the pro-inflammatory markers TNF-α, CCL2, CD11b and TREM-1 were evaluated by Real-Time PCR in the liver of wild-type and ICOS$^{-/-}$ mice at different time points following the administration of CCl_4. The results are expressed as mean ± SD of 5-8 animals for each time point. The vertical boxes indicate statistically significant differences between wild-type and ICOS$^{-/-}$ mice at each time point.

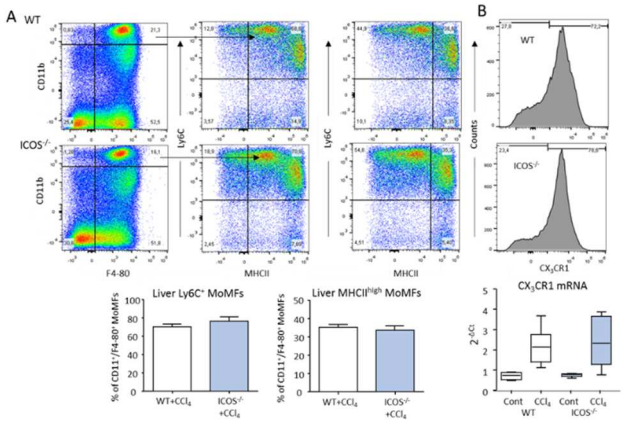

Figure 6: ICOS deficiency does not interfere with the recruitment and maturation of inflammatory MoMFs in response to acute liver injury.

Wild-type and ICOS$^{-/-}$ mice received CCl_4 for 24 hours. (Panel A) The expression of Ly6C^{high} and MHCII was monitored by flow cytometry in liver CD11b^{high}/F4-80^{+} MoMFs. (Panel B) The expression of CX_3CR1 was evaluated by Real-Time PCR as well as by MoMF flow cytometry in the liver of wild-type (WT) and ICOS$^{-/-}$ mice 24 hours following the administration of CCl_4. The values are expressed as mean ± SD of three different cell preparations or 5-6 animals.

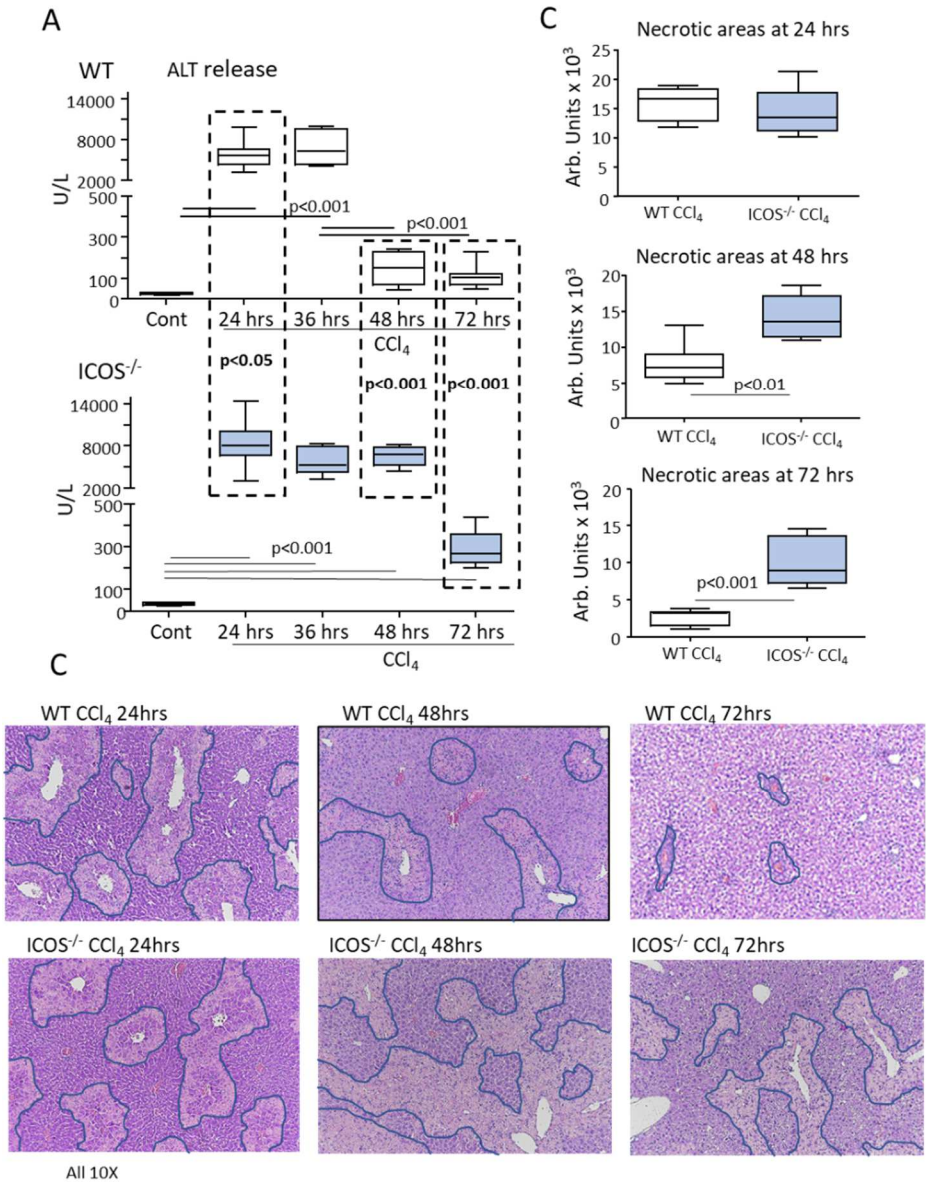

Figure 7: ICOS deficiency impairs the resolution of acute liver injury.

The evolution of acute liver injury induced by the administration of CCl_4 in wild-type and *ICOS*$^{-/-}$ mice was monitored by measuring alanine aminotransferase (ALT) release (Panel A) and by morphometric evaluation of necrotic areas (encircled by blue lines) in liver sections stained with hematoxylin/eosin (magnification 10X)(Panels B and C). The results are expressed as mean ± SD of 5-8 animals for each time point.

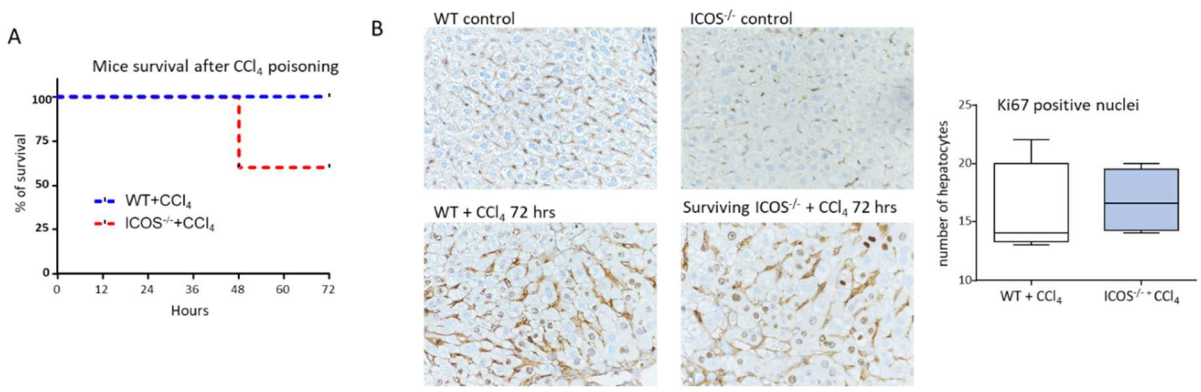

Figure 8: **ICOS deficiency enhances mice mortality following CCl_4 poisoning without affecting hepatocyte replicative capability.**

Wild-type and $ICOS^{-/-}$ mice received CCl_4 for 24-72 hours. (Panel A) Kaplan-Mayer curve for hepatocyte survival following CCl_4 poisoning. (Panel B) Nuclear hepatocyte staining with the proliferation marker Ki67 was evaluated in paraffin fixed liver sections and the number of Ki67 positive nuclei was evaluated in five randomized areas. The results are expressed as percent of all nuclei and are means ± SD of 3-4 representative animals. Magnification 40X.

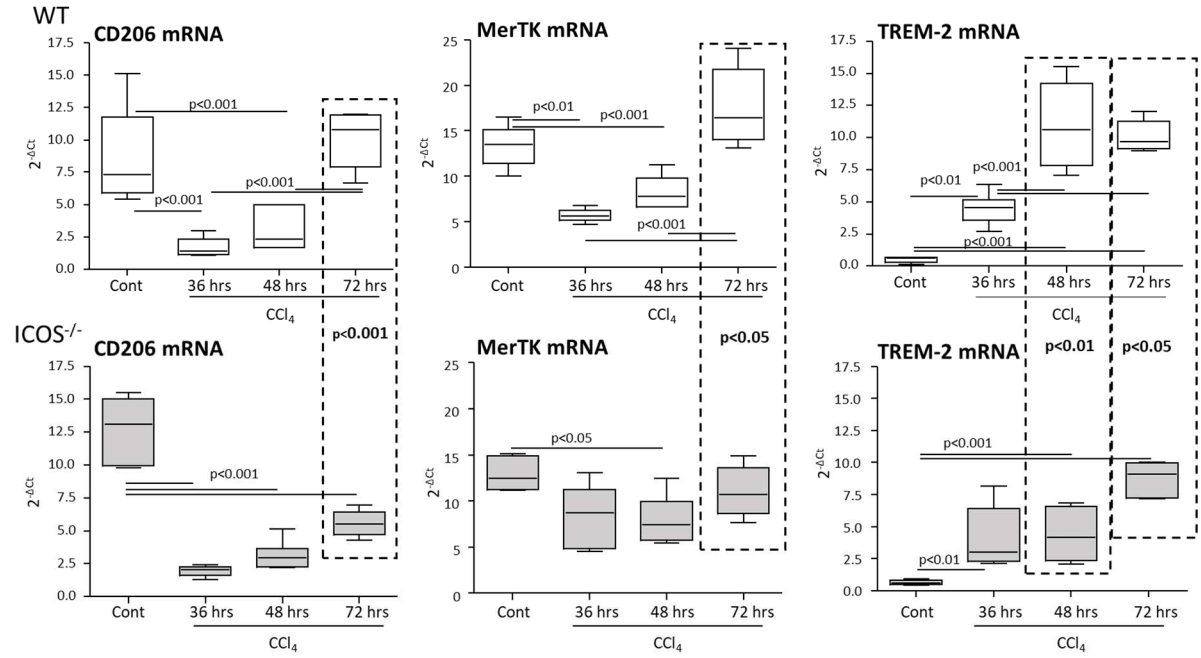

Figure 9: ICOS deficiency impairs the expression of reparative MoMF markers during the evolution of acute liver injury.

The transcripts of reparative MoMF markers CD206, MerTK, and TREM-2 were evaluated by Real-Time PCR in the liver of wild-type and *ICOS*$^{-/-}$ mice at different time points following the administration of CCl_4. The vertical dotted boxes indicate statistically significant differences between wild-type and *ICOS*$^{-/-}$ mice at each time point. The results are expressed as mean ± SD of 5-8 animals for each time point.

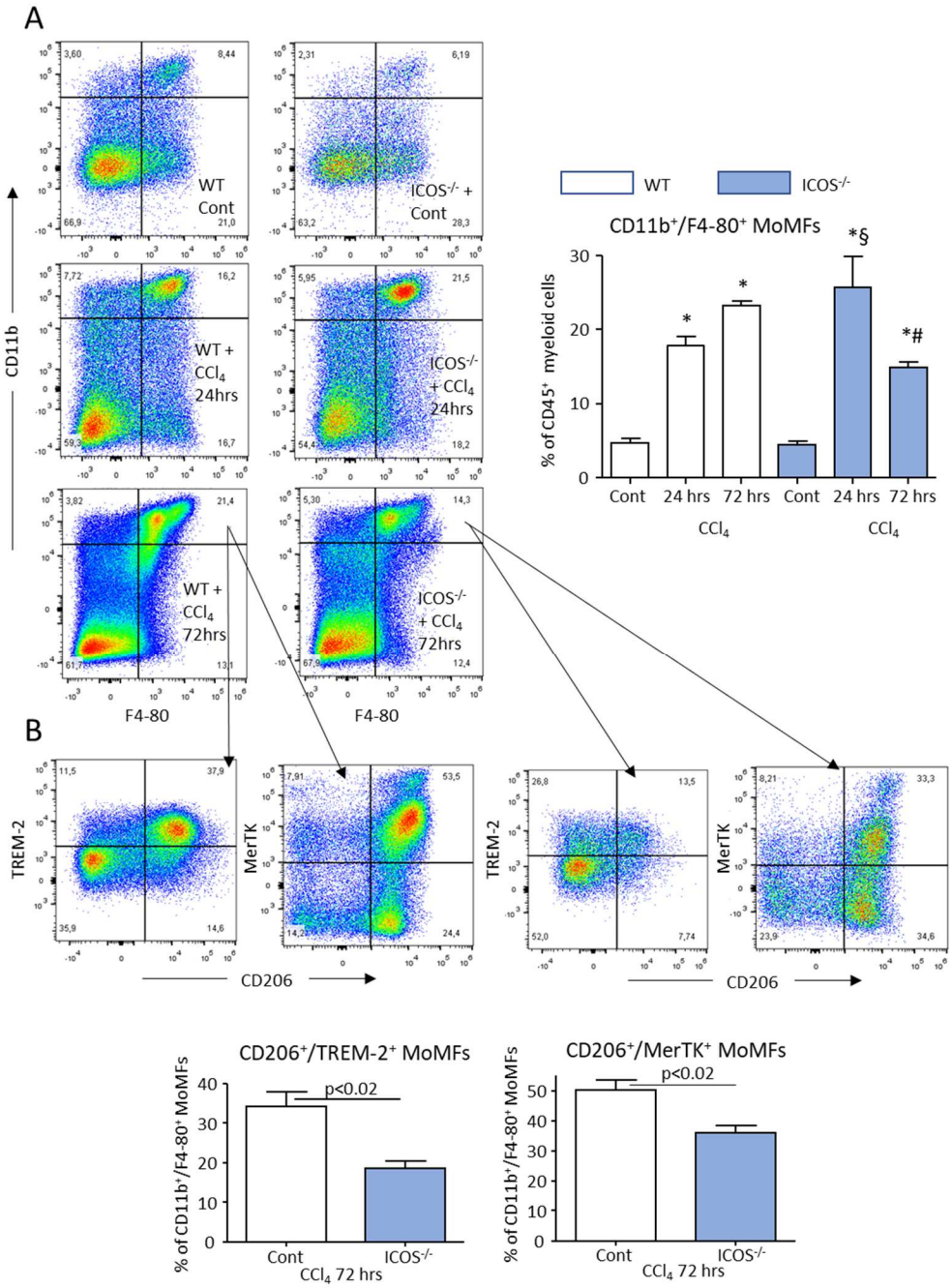

Figure 10: ICOS deficiency causes the loss of reparative MoMFs during the resolution of acute liver injury.

The prevalence of liver CD11b$^+$/F4-80$^+$ MoMFs during the evolution of acute liver injury induced in wild-type and *ICOS*$^{-/-}$ mice receiving CCl_4 was monitored by flow cytometry 24 or 72 hours after challenge with the toxic agent (Panel A). Characterization of the co-expression of CD206, TREM-2 and MerTK among CD11b$^+$/F4-80$^+$ MoMFs infiltrating the liver during the resolution of acute liver damage (Panel B). The results are expressed as mean ± SD of 3-4 different cell preparations.

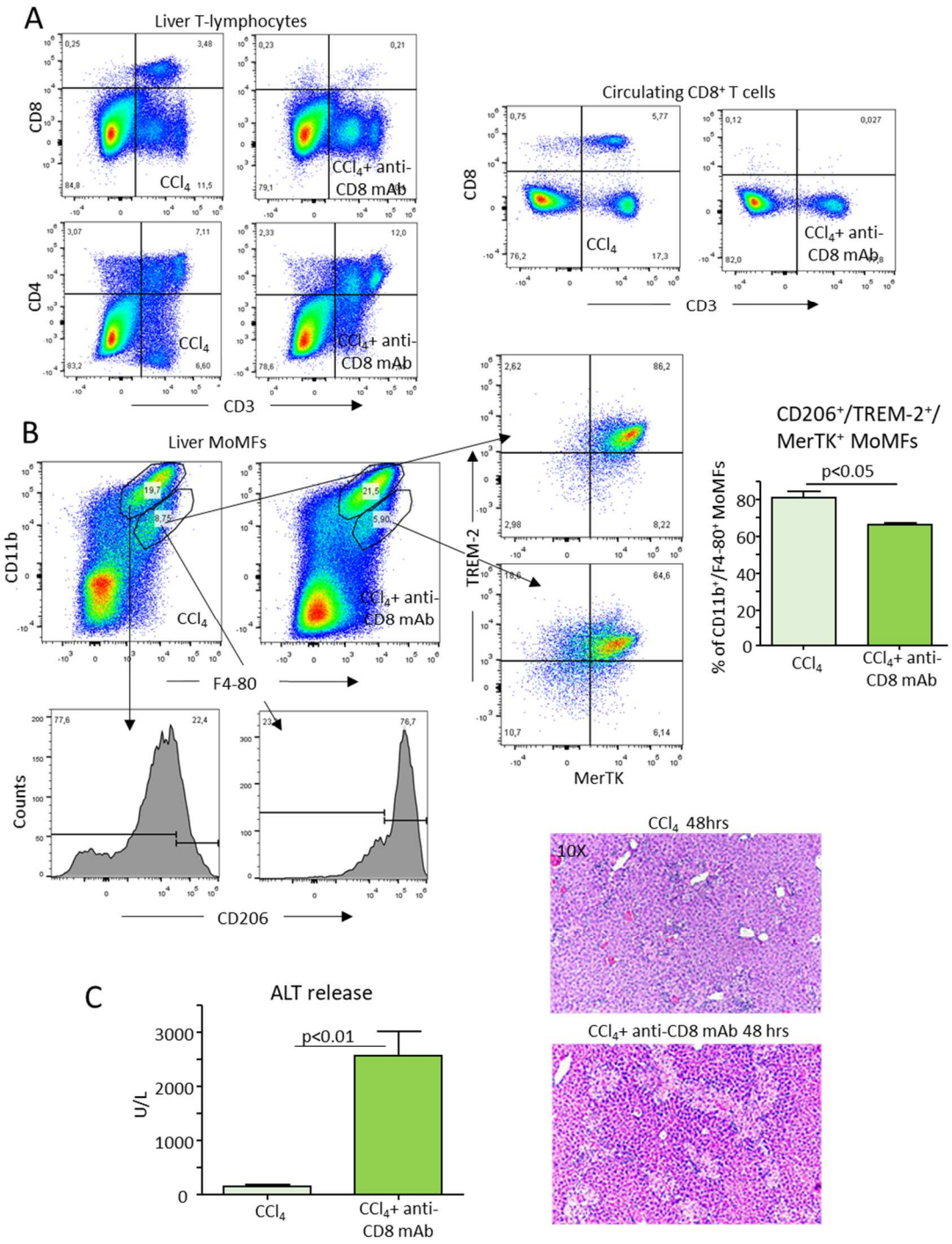

Figure 11: Depletion of CD8⁺ T-lymphocytes lowers reparative MoMFs and impairs the resolution of acute liver injury.

Mice were treated with an anti-CD8 monoclonal antibody (mAb) 72 hours before and immediately after CCl_4 administration and the evolution of hepatic injury was evaluated 48 hours after CCl_4 poisoning. The distribution of liver and circulating $CD4^+$ and $CD8^+$ T cells and that of hepatic $CD11b^+/F4\text{-}80^+$ MoMFs was monitored by flow cytometry in mice receiving CCl_4 (Panel A). The lowering of $CD11b^+/F4\text{-}80^+$ MoMFs induced by CD8 T-cell ablation involved CD206, TREM-2 and MerTK-expressing cells (Panel B). The effects of $CD8^+$ T-depletion of the recovery

from acute liver injury was evaluated by measuring alanine aminotransferase (ALT) release and histological analysis of liver sections stained with hematoxylin/eosin (magnification 10X) (Panel C).

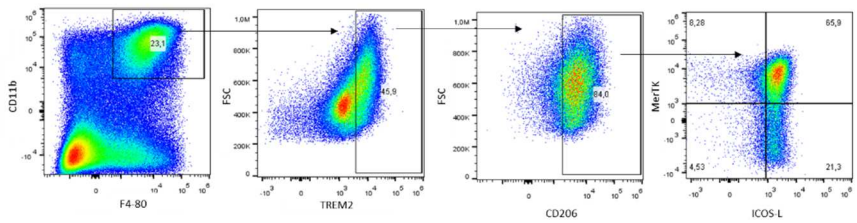

Figure 12: Reparative MoMFs express ICOS-L.

The expression of ICOS-L was evaluated by flow cytometry in TREM-2^{+}, CD206^{+}, MerTK^{+} and reparative CD11b^{+}/F4-80^{+} MoMFs isolated from the liver of a wild-type mice.

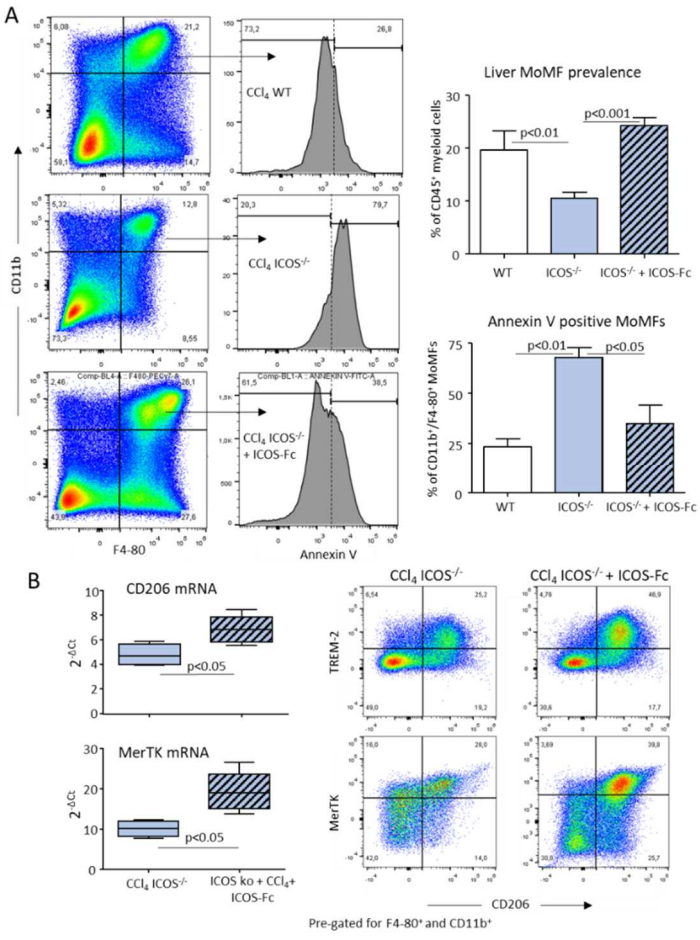

Figure 13: **ICOS modulates the survival of reparative MOMFs during the resolution of acute liver injury.**

Annexin V staining of apoptotic CD11b^{+}/F4-80^{+} MoMFs and the overall MoMF prevalence were evaluated by flow cytometry in the liver of wild-type and *ICOS*$^{-/-}$ mice 72 hours after receiving CCl_4 in combination or not with recombinant ICOS-Fc treatment (Panel A). Real-Time PCR analysis of the hepatic transcripts for CD206 and

MerTK in ICOS$^{-/-}$ mice receiving CCl_4 for 72 hours with or without ICOS-FC supplementation (Panel B). Hepatic distribution of CD206^{+}/TREM-2^{+}/MerTK^{+} reparative MoMFs in ICOS$^{-/-}$ mice receiving CCl_4 for 72 hours with or without ICOS-Fc supplementation (Panel C). The results are expressed as mean ± SD of 3-4 different cell preparations of 5-6 mice.

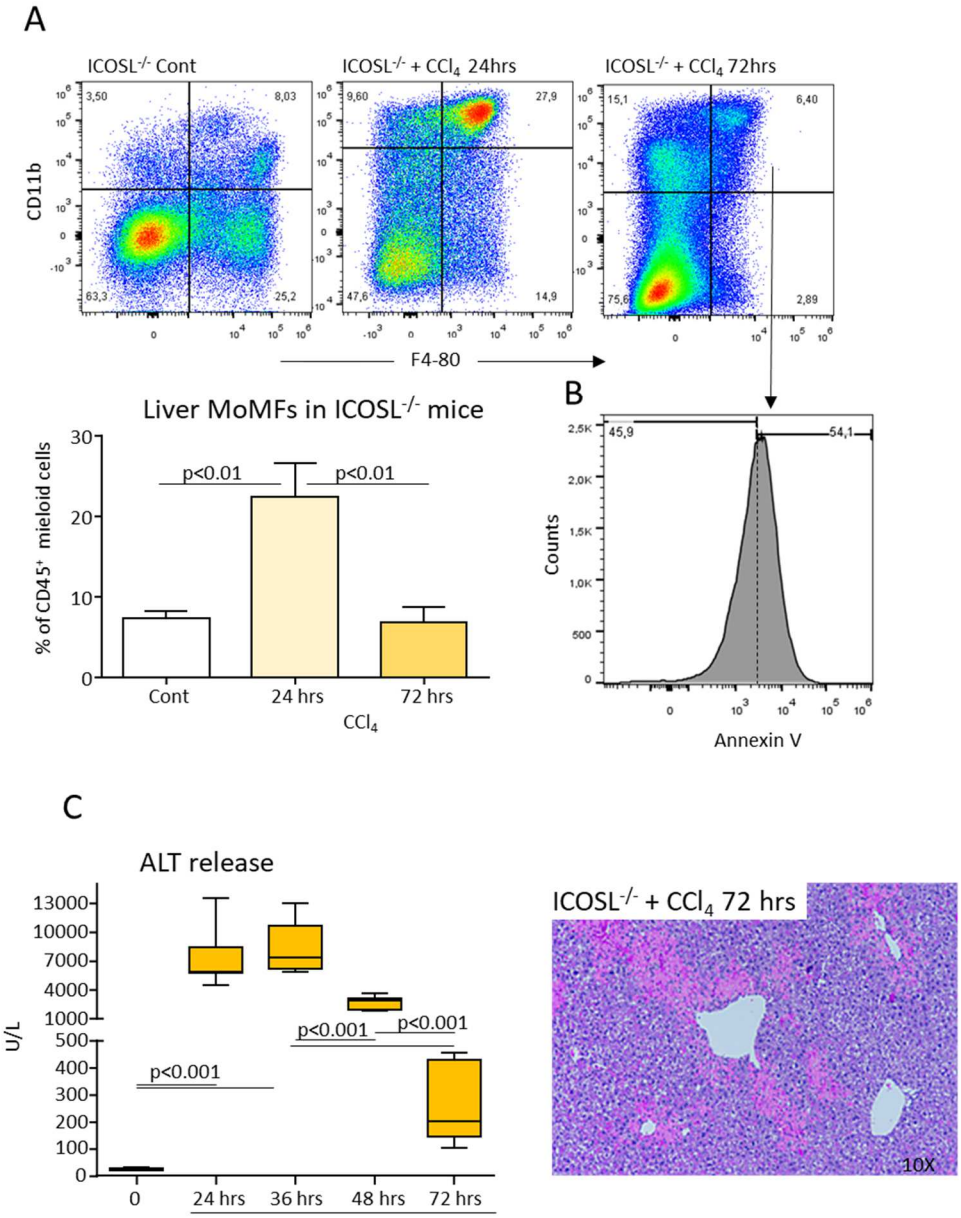

Figure 14: ICOSL deficiency of impairs MoMF survival and liver healing following acute liver injury.

Wild-type and *ICOSL*$^{-/-}$ mice received CCl_4 for 72 hours. The liver prevalence of MoMFs (Panel A) and the expression of the apoptosis marker annexin V (Panel B) were evaluated by flow cytometry. The evolution of liver damage was monitored by circulating alanine aminotransferase (ALT) and liver histology of liver sections stained with hematoxylin/eosin (magnification 10X) (Panel C). The results are expressed as mean ± SD of 3-5 animals for each time point.

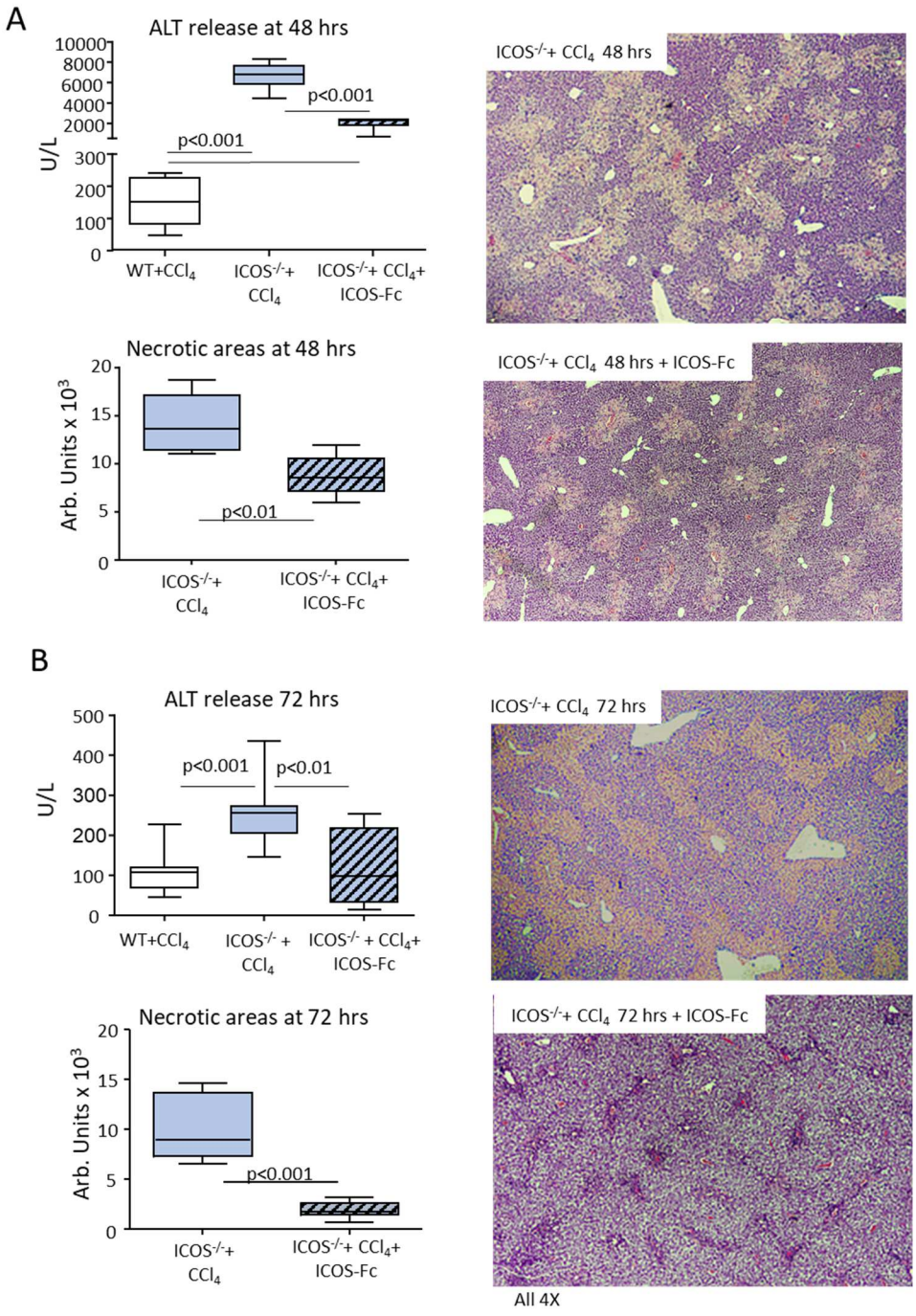

Figure 15: Mice supplementation with recombinant ICOS improves the recovery from acute liver injury.

Wild-type and ICOS$^{-/-}$ mice received CCl_4 for 48 (Panel A) or 72 hours (Panel B) and the recovery from liver injury was evaluated by measuring alanine aminotransferase (ALT) release and by morphometric evaluation of necrotic areas in liver sections stained with hematoxylin/eosin (magnification 4X). The results are expressed as mean ± SD of 5-6 animals for each time point.

4.4) Discussion

It is now well established that during the evolution of acute liver injury the phenotype switching of Ly6C^{high} pro-inflammatory MoMFs to Ly6C^{low} reparative MoMFs is critical for effective healing of parenchymal damage (Wen Y et al. 2021)**.** Reparative MoMFs are, in fact, responsible for clearing death cells and cellular debris, remodeling extracellular matrix and producing cytokines and growth factors involved in promoting hepatocyte proliferation, such as IL-6, hepatocyte growth factor (HGF) and insulin-like growth factor (IGF) (Wen Y et al. 2021). Recent studies have shown that the reprogramming of liver MoMFs to the reparative phenotype involves IL-4 released by basophils and invariant natural killer T (iNKT) cells, as well as signals transduced by MerKT and TREM-2 receptors (Wen Y et al. 2021; Coelho I et al. 2021; Triantafyllou E et al. 2018). Here, we show that beside these mechanisms, effective repair of acute liver damage also requires the presence of $CD8^+$ T-lymphocytes expressing the co-stimulatory molecule ICOS. In fact, the deficit of ICOS, ICOS-L or $CD8^+$ T-cells impairs the complete clearing of centrilobular necrosis 48-72 hours from acute liver damage induced by CCl_4 poisoning. This effect is associated with an increase in parenchymal infiltration by granulocytes and an enhanced mortality of mice by acute liver failure.

Although the best characterized function of ICOS/ICOSL dyad is triggering ICOS on T-cells (Sakai M 2019), growing evidence indicates that following the interaction with ICOS also ICOSL can transduce “reverse signals” in ICOSL expressing cells. ICOSL is constitutively present on antigen presenting cells (APCs) such as dendritic cells, macrophages, and B-lymphocytes as well as on some non-lymphoid cells, such as endothelial cells and several tumour cells (Wikenheiser DJ et al. 2016; Dianziani C et al. 2010; Dianziani C et al. 2014). In either human umbilical vein endothelial cells, dendritic cells and tumour cell lines ICOSL stimulation impairs the adhesive and migratory capacities (Dianziani C et al. 2010; Dianziani C et al. 2014), while it modulates cytokine secretion and antigen presentation by monocyte-derived dendritic cells (Tang Get al. 2009; Occhipinti S et al. 2013). Furthermore, ICOSL signalling prevents the differentiation of monocyte to osteoclasts stimulated by receptor activator of NF-kB ligand (RANKL) (Gigliotti CL et al. 2016). This latter effect involves the specific stimulation of p38 mitogen activated kinase (Gigliotti CL et al. 2016), while the action in dendritic cell depends upon JNK and PKC transduction (Occhipinti S et al. 2013). Interestingly, ICOSL interaction with

$\alpha_v\beta_3$ integrin also modulates podocyte adhesion and ICOSL$^{-/-}$ mice are more susceptible to proteinuria induced by endotoxin treatment or diabetic nephropathy (Koh KH et al. 2019).

We have shown that within the liver, ICOSL is mainly expressed by CD11b^{high}/F4-80^{+} MoMFs recruited in response to parenchymal injury as well as by CD206^{+}/MerKT^{+}/TREM-2^{+} MoMFs associated with healing from acute damage. This is consistent with an early report showing that, differently from lung epithelial cells, hepatocytes did not express ICOSL (Wah CH et al. 2008). In line with the capacity of ICOSL-mediated signals of influencing monocyte-derived cells, we have observed that ICOS/ICOSL interaction is required for the survival of reparative MoMFs during the healing phase. In fact, both ICOS and ICOSL deficient mice show an enhanced rate of MoMF apoptosis 72 hours after CCl_4, which can be rescued by the administration of soluble ICOS-Fc to ICOS$^{-/-}$ mice. Mice treatment with ICOS-Fc also allows the full clearance of centrilobular necrosis. The involvement of MoMFs expressing MerKT and TREM-2 receptors in the recovery from acute liver injury is consistent with the notion that both MerKT or TREM-2 are required for damping macrophage pro-inflammatory functions and promoting the clearance of apoptotic cells (Coehl I et al. 2021; Triantafyllou E et al 2018; Perugorria MJ et al. 2019). Moreover, recent reports have shown that mice deficient in either MerKT or TREM-2 suffer a delayed resolution of acetaminophen hepatotoxicity (Coehl I et al. 2021; Triantafyllou E et al 2018; Perugorria MJ et al. 2019). Interestingly, the expansion of MerTK-positive MoMFs is also evident in the liver of patients with acute liver failure and associates with a greater severity of liver injury and adverse clinical outcome (Perugorria MJ et al. 2019).

At present, the network of signals that promotes the survival of reparative MoMFs has not been investigated in detail. Previous studies have shown that early after infiltrating injured liver MoMFs up regulate the fractalkine receptor CX_3CR1 as well as MerTK, both of which are involved in regulating their survival (Sutti S et al. 2017; Perugorria MJ et al. 2019).

In our hands, the expression of CX_3CR1 is unaffected in MoMFs from *ICOS*$^{-/-}$ mice, which instead show reduced MerTK transcripts. These data and the observation that reparative MoMFs are greatly lowered in the liver of MerTK-deficient mice during the recovery from acetaminophen poisoning (Perugorria MJ et al. 2019) suggest the possibility that ICOS/ICOSL interaction might contribute to MerTK-mediated signals. Nonetheless, we cannot exclude

that other receptor including TREM-2 might also be implicated, since TREM-2 is required for the survival of liver MoMFs and brain microglial cells (Coehl I et al. 2021; Zheng H et al. 2017).

The involvement of ICOS/ICOSL dyad in liver repair is consistent with the report by Maeda and colleagues of a dramatic delay in skin wound healing in both *ICOS*$^{-/-}$ and *ICOSL*$^{-/-}$ mice (Maeda S et al. 2011). They observed that in both strains impaired wound healing associates with a strong reduction in keratinocyte migration, angiogenesis, and granulation tissue formation, as well as with a reduced wound infiltration by T-cells, macrophages, and neutrophils. These effects were mimicked by whole T-cell depletion, suggesting that signals involving ICOS were driving skin healing. However, in this setting, the supplementation with $CD4^+$ T cells and IL-6 improved epidermis repair (Maeda S et al. 2011).

A further novel aspect emerging from this study regards the involvement of $CD8^+$ T lymphocytes in the regulation of hepatic repair. So far, the role of lymphocytes in the evolution of acute liver injury has been incompletely characterized. The available evidence indicates that liver recruitment of B and T cells accompanies that of granulocytes and MoMFs following ischemia/reperfusion or acetaminophen poisoning (Zwacka RM et al. 1997; Khandoga A et al. 2006; Puengel T et al. 2017). However, while $CD4^+$ T helper cells contributes to ischemia/reperfusion liver damage likely by stimulating MoMFs via CD40/CD154 co-stimulatory molecules and interferon-γ secretion (Puengel T et al. 2017; Ke B et al. 2005), their role in other type of acute liver damage has not been investigated in detail. Here, we show that $CD4^+$ and $CD8^+$ T-cells are recruited within the liver in response to CCl_4-induced hepatocyte injury and that $CD8^+$ T-cells support the recovery phase by providing ICOS-mediated survival signals to reparative $CD206^+$/$MerKT^+$/$TREM\text{-}2^+$ MoMFs. Previous studies have shown that regulatory T-cells (Tregs), promote repair and regeneration of various organs (Zhang C et al. 2017). Furthermore, Liew and co-workers have recently reported that iNKT cells secreting IL-4 are important in liver repair by stimulating MoMF phenotype switching (Liew PX et al. 2017). Our data are not in contrast to these observations but add further complexity to the mechanisms responsible for driving liver repair. Recent data indicate that IL-2-producing tissue resident/memory $CD8^+$ T-cells are present within the liver where they patrol the vasculature and provide protection against invading pathogens (Pallett LJ et al. 2017). Thus, it is possible that, in response to an inflammatory environment, these cells up-regulate ICOS allowing them to stimulate $ICOSL^+$ MoMFs. The involvement of direct cellular

interaction in modulating liver MoMF functions is in line with a recent report by Sakai and co-workers (Sakai M et al. 2019) showing that the Notch and transforming growth factor-β family ligands produced by sinusoidal endothelial cells are required for inducing MoMF differentiation to Kupffer cells. However, further studies are required to better characterize the transcriptional changes associated with MoMF/$CD8^+$ T-cells interaction within the liver also considering that single cells RNA-sequencing of cells obtained from livers of human cirrhotic patients has identified TREM-2/CD9 expressing MoMFs in the fibrotic niches (Ramachandhran P et al. 2019).

In conclusion, our data demonstrated that MoMF interaction with $CD8^+$ T-lymphocytes through the ICOS/ICOSL dyad plays an important role in liver healing after acute injury by supporting the survival of reparative MoMFs. These observations open the possibility of targeting ICOSL as a novel tool to promote healing responses following acute liver injury.

5.Results Section 2

Annexin A1 treatment prevents the evolution to fibrosis of experimental nonalcoholic steatohepatitis (NASH)

Data submitted to Clinical Sciences

5.1 Foreword

Nonalcoholic steatohepatitis (NASH) is now becoming one of the most common causes of end-stage liver disease in western countries with a death rate ascribed to NASH-related cirrhosis accounting for 12-25% (Younossi Z et al. 2018; Lindenmever CC et al. 2018). NASH is also an increasingly common cause of hepatocellular carcinoma (HCC) (Younes R et al. 2017). Beside hepatic injury, the presence of steatohepatitis also increases the prevalence of non-hepatic diseases such as type 2 diabetes mellitus, cardiovascular diseases, chronic kidney diseases and osteoporosis independently from the risk factors in common with metabolic syndrome (Amstrong MJ et al. 2014). In these settings, liver inflammation not only is the driving force for NASH evolution to cirrhosis, but also contributes to extrahepatic injury. Thus, targeting hepatic inflammation has become an important objective for the development of new treatments of NASH. Animal experiments and clinical trials have shown that interfering with pro-inflammatory cytokines/chemokines, leukocyte adhesion molecules or gut dysbiosis is effective in ameliorating lobular inflammation and NASH progression to fibrosis (Rotman Y et al. 2017; Reimer KC et al. 2020). A different approach to control inflammation might rely on the use of physiological modulators that orchestrate the resolution of inflammatory processes and promote tissue healing (Serhan CN et al. 2017). Among these pro-resolving factors, Annexin A1 (AnxA1), also known as lipocortin-1, represents a possible candidate.

AnxA1 is a 37-kDa calcium-phospholipid–binding protein highly expressed in myeloid cells and regulated by glucocorticoids [8]. AnxA1 interaction with its receptor, formyl peptide receptor 2/lipoxin A4 receptor (FPR2/ALX), down-regulates the production of proinflammatory mediators, such as eicosanoids, nitric oxide and interleukin-6 (IL-6), reduces neutrophil migration to inflammatory sites, and promotes clearance of apoptotic

granulocytes (Suigimoto MA et al.2016; Sheikh MH et al. 2018). Furthermore, recent studies showed that endogenous AnxA1 favor epithelial repair and muscle regeneration (Sheikh MH et al. 2018; McArthur S et al.2020). We have observed that AnxA1 is selectively upregulated in macrophages from mouse and human NASH livers (Locatelli I et al. 2014). Moreover, in NASH patients hepatic AnxA1 transcripts show an inverse correlation with disease progression to fibrosis/cirrhosis (Locatelli I et al. 2014). Furthermore, AnxA1 deficiency enhances insulin resistance and metabolic impairment in mice receiving an obesogenic diet (Purvis GSD et al. 2019), while it worsens lobular inflammation and hepatic fibrosis in experimental NASH (Locatelli I et al. 2014). These latter effects associate with an enhanced macrophage recruitment as well as their pro-inflammatory M1 phenotype and activity (Locatelli I et al. 2014). Consistently, in vitro addition of recombinant AnxA1 to macrophages isolated from NASH livers reduces M1 polarization by stimulating the production of interleukin-10 (Locatelli I et al. 2014). In the same vein, AnxA1 supplementation improves insulin resistance and type 2 diabetes complications in mice fed with a high fat diet (Purvis GSD et al. 2019).

Based on these studies and the recent observations that AnxA1 and AnxA1 mimetic peptides are effective in improving inflammation in animal models of diabetic kidney damage and atherosclerosis (Wu L et al. 2021; Kusters DHM et al. 2015), the present study investigated the possible application of AnxA1 in controlling steatohepatitis in mice with experimental NASH.

5.2 Experimental data

a) Human recombinant Annexin A1 prevents steatohepatitis and fibrosis in mice.

The effects of human recombinant AnxA1 (hrAnxA1) on modifying the severity of NASH were preliminary evaluated in a set of experiments in which extensive steatohepatitis was induced in C57BL/6 mice by feeding a diet deficient in methionine and choline (MCD). For these experiments, animals received the MCD diet for 4 weeks to allow the development of extensive steatohepatitis; then, they were injected with hrAnxA1 or saline for further 4 weeks, while maintaining the same diet. At the end of the treatment, liver histology and biochemical analysis showed that administration of hrAnxA1 significantly reduced the severity of liver injury (Fig. 1A) as measured by alanine aminotransferase (ALT) release (Fig. 1B). No changes were evident in the scores for hepatic steatosis (2.2±0.9 *vs.* 1.6±0.6 arbitrary units; n=13; p=0.22) and in liver triglyceride content (Fig. 1C). The same animals also showed a significant lowering in the histological scores for lobular inflammation (2.2±0.8 *vs.* 0.8±0.8 arbitrary units; n=13; $p<0.05$) as well as in the liver expression of pro-inflammatory markers like Tumor Necrosis Factor-α (TNF-α), CCL2, IL-12p40 and the leukocyte marker integrin alpha M (ITGAM; CD11b) (Fig. 1D-G). Steatohepatitis in mice receiving the MCD diet for 8 weeks increased liver transcripts for procollagen-1 α and transforming growth factor 1β (TGF-1β) (Fig. 2 A-C) and the onset of liver fibrosis, as evidenced by intra-hepatic collagen staining with Sirius Red (Fig. 2C). Interestingly, mice treated with hrAnxA1 showed significant decrease in the transcripts for procollagen-1α and TGF-1β (Fig.2A-B), along with a lower Sirius Red staining, than those injected with saline alone (Fig. 2C).

Although steatohepatitis induced by the MCD diet reproduces the inflammatory features of human NASH, this experimental model lacks metabolic derangements associated with obesity and insulin resistance that are common features of the human disease (Santhikadhur PK et al. 2018). Furthermore, the development of fibrosis is usually modest in MCD-fed mice (Santhikadhur PK et al. 2018). Thus, to better characterize the action of hrAnxA1 on the evolution from NASH to fibrosis, we switched to a nutritional model based on mice feeding with high-fat/carbohydrate diet enriched with 1.25% cholesterol known as Western Diet (WD) (Santhikadhur PK et al. 2018).

To this aim, mice were fed with WD for 10 weeks to induce steatohepatitis before being randomized to receive hrAnxA1 supplementation. Preliminary experiments confirmed that 10 weeks feeding of mice with WD significantly increased body weight as compared to chow-fed controls and this associated with an increase in liver weight due to intrahepatic fat accumulation (Fig. 3A). The presence of steatohepatitis was confirmed by histology (Fig. 3B) as well as elevation in the circulating levels of ALT (Fig. 3C) and in the liver transcripts for inflammatory markers (Supplementary Fig. 3D, 3E). Although procollagen-1α mRNA was increased in the livers of WD-fed mice (Supplementary Fig. 3F), histology did not detect changes in collagen deposition (Fig. 3G), suggesting that at this time point steatohepatitis has not led to marked fibrosis. Thus, 10-week WD-fed animals were a suitable experimental model to investigate whether treatment with hrANXA1 might interfere with NASH evolution to fibrosis.

Six weeks treatment with hrANXA1 (1 μg/g) of mice receiving WD did not appreciably modify body (33±1.8 g *vs.* 32.5±2.6 g; n=12; p=0.7) and liver weights (2.3±0.32 g *vs.* 2.0±0.32 g; n=12; p=0.12). As expected, 16-week WD feeding promoted the development of insulin resistance, as monitored through the glucose tolerance test (Fig. 4B). Nonetheless, the area under the curve (AUC) did not evidence an appreciable improvement of insulin response following administration of hrANXA1 (Fig. 4A).

As observed in the animals receiving the MCD diet, hrANXA1 treatment of mice fed with WD improved liver histology (lobular inflammation score: 1.8±0.4 *vs.* 0.8±0.7 arbitrary units; n=12; p<0.05) (Fig. 5A), transaminase release (Fig. 5B) and expression of inflammatory markers (Fig. 5D, 5E), without affecting the extension of steatosis (2.0±0.9 *vs.* 2.3±0.8 arbitrary units; n=12; p=0.58). According to previous studies (Santhekadur PK et al. 2018), WD administration led to diffuse hepatic fibrosis (Fig. 2D-F). In these animals RT-PCR and Sirius Red collagen staining confirmed that hrANXA1 was effective in preventing the up-regulation in procollagen-1α (Fig. 2D)and TGF-1β (Fig. 2E) expression and almost abrogated intra-hepatic collagen deposition (Fig. 2F) as confirmed by morphometric evaluation of collagen Sirius Red staining areas (3.20±0.93% *vs.* 0.35±0.35% n=23 fields; p<0.001).

b) Annexin A1 modulates liver macrophage phenotype

Several reports have pointed on the capacity of ANXA1 to modulate macrophage functions by suppressing pro-inflammatory activities and stimulating pro-resolving functions (Sugimoto MA et al. 2016; Sheikh MH et al. 2018). In our hands, flow cytometry analysis of F4-80$^+$/CD11b$^+$ monocyte/macrophages (MoMFs) infiltrating the liver showed that treatment with hrANXA1 did not interfere with the recruitment of monocytes to the liver (Fig. 6). Similarly, the fraction of pro-inflammatory MoMFs expressing the lymphocyte antigen 6 (Ly6C), also known as tissue plasminogen activator receptor (Wen Y et al. 2020), was not affected (Fig. 6). On the other hand, hrANXA1 reduced by ~20% the prevalence of MoMFs expressing the mannose-binding protein receptor (MRC1; CD206), a marker of reparative macrophages (Fig. 6). In recent studies, single-cell RNA sequencing of liver macrophage has revealed that MoMFs expanding in either human and rodent NASH, also called NASH-associated macrophages (NAM), have a specific phenotype, characterized by the expression of the Triggering Receptor Expressed on Myeloid cells 2 (TREM-2), CD63 and the glycoproteins CD9 and NMB (GPNMB). In humans NAM prevalence correlates with the severity of NASH (Itoh M et al. 2013), likely in relation to their capability of producing pro-fibrogenic mediators such as osteopontin (OPN) and galectin-3 (Gal-3) (Itah M et al. 2013; Xiong X et al. 2019; Seidman JS et al. 2020; Remmerie A et al. 2020). Furthermore, NAMs appeared to be the main components of crown-like macrophage aggregates (Remmerie A et al. 2020), that characterize both human and rodents NASH (Daemen S et al. 2021). Since the worsening of NASH-associated fibrosis in AnxA1-deficient mice was characterized by an enhanced production of Gal-3 by macrophages in crow-like structures (Locatelli I et al. 2014), in subsequent experiments we investigated the possibility that the protection against fibrosis observed in hrANXA1-treated mice might be related to an action on NAMs. Analysis of TREM-2, OPN and Gal-3 transcripts confirmed a strong up-regulation of these NAM markers in the livers of mice receiving WD that was effectively prevented by the administration of hrANXA1 (Fig. 7 A-C). Moreover, immunohistochemistry of NASH liver sections for Gal-3 showed an increased staining selectively in macrophages within crown-like aggregates; again, this effect was greatly reduced by the treatment with hrANXA1 (Fig. 7D). Such an action associated with a reduction in the prevalence of crown-like aggregates as confirmed by immunostaining with the macrophage marker F4-80 (Fig. 7E).

c. Annexin A1 modulates the differentiation of NASH associated macrophages.

From the above results, and previous observations showing that macrophages in crown-like aggregates in both rodent and human NASH produce AnxA1(Locatelli I et al. 2014; Jindal A et al. 2015), we postulated that AnxA1 might act in a paracrine manner in modulating the phenotype of hepatic MoMFs. To verify such a possibility, we evaluated the effects of hrANXA1 on the differentiation of TREM-2^{+}/CD9^{+} NAMs in mice receiving the MCD diet for 2 weeks. Preliminary experiments have shown that the early stages of steatohepatitis in these animals are accompanied by an expansion of F4-80^{+}/CD11b^{+} MoMFs which included about 40% of cells that were Ly6C^{-}/TREM-2^{+}/CD9^{+}/CD206^{high} (Fig. 8). In further experiments, during the second week on the MCD diet, mice were injected with hrANXA1 or saline for 5 days: herein, we observed that administration of hrANXA1 to mice did not affect the extent of MoMF recruitment, but significantly lowered the fraction of TREM-2^{+}/CD206^{+} cells (Fig. 9), supporting the possibility that hrANXA1 prevents NASH evolution to fibrosis by interfering with NAM phenotype in macrophages.

5.3 Figures Section 2

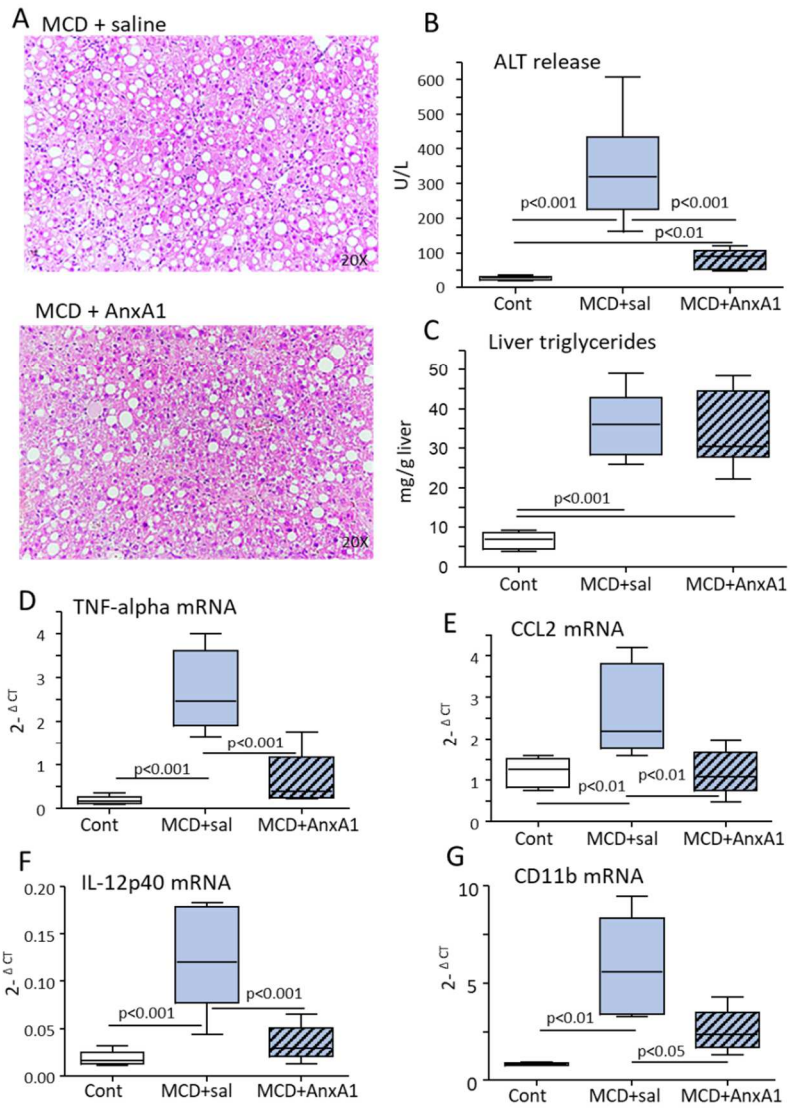

Figure 1: Annexin A1 (AnxA1) supplementation improves NASH-associated hepatic injury and inflammation in mice fed with a methionine/choline deficient (MCD) diet.

NASH was induced in wild type C57BL/6 mice by feeding MCD diet for 4 weeks. The animals were then randomly divided in two groups one receiving AnxA1 (1 µg/daily in saline 5 time a week)(MCD+AnxA1) and the other the same volume of saline (MCD+sal) and the administration of the MCD diet was continued for further 4 weeks. (Panel A) Hematoxylin/eosin staining of liver sections (magnification 20x). (Panels B,C) Alanine aminotransferase (ALT) release and hepatic triglyceride content. (Panels D-G) Hepatic transcripts of inflammatory markers TNF-α, CCL2, IL12p40 and CD11b as evaluated by RT-PCR. The values refer to 6-8 animals per group and the boxes include the values within 25th and 75th percentile, while the horizontal bars represent the medians. The extremities of the vertical bars (10th-90th percentile) comprise 80% percent of the values.

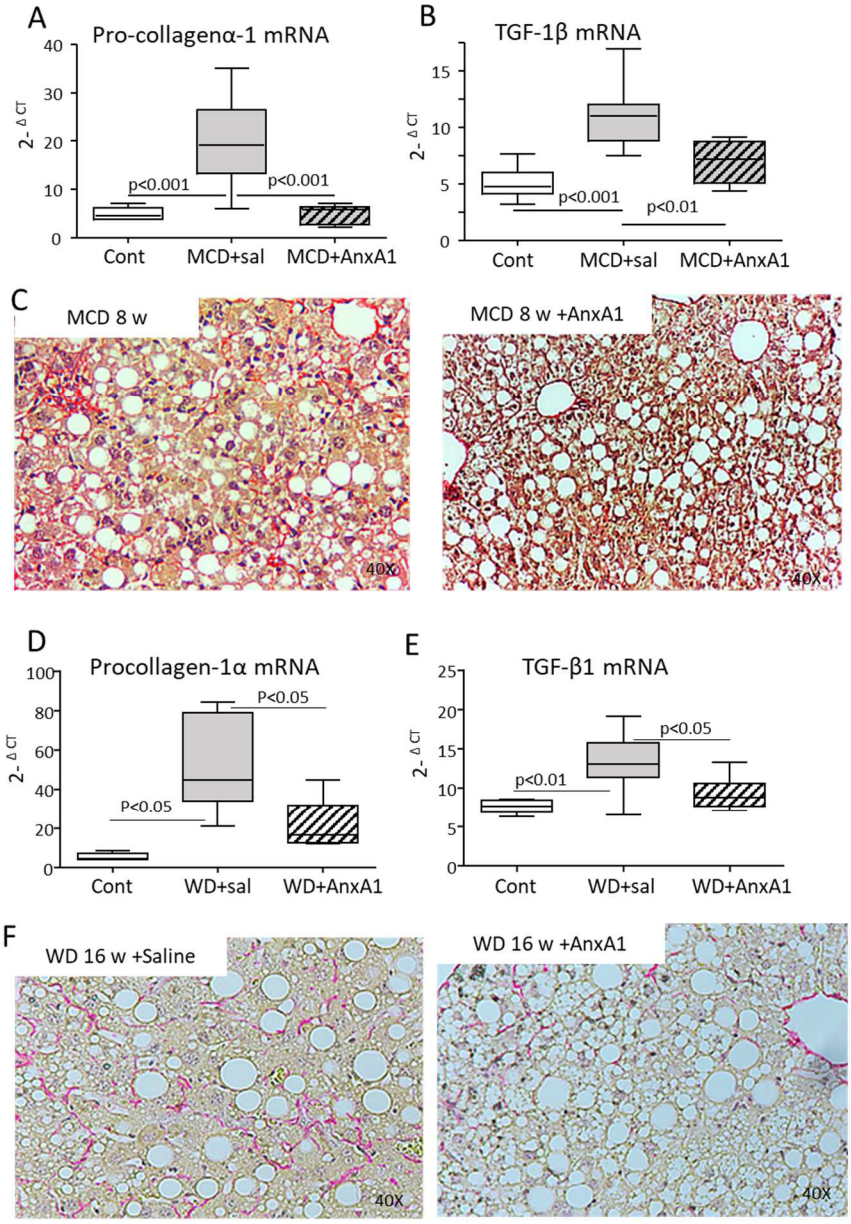

Figure 2: **Annexin A1 (AnxA1) supplementation improves hepatic fibrosis in mice with NASH induced by feeding either a methionine/choline deficient (MCD) diet or WD diet.**

NASH was induced in wild type C57BL/6 mice by feeding MCD diet for 4 weeks or WD diet for 10 weeks. (Panels A-C) The animals were randomly divided in two groups one receiving AnxA1 (1 µg/daily in saline 5 time a week) (MCD+AnxA1) and the other the same volume of saline (MCD+sal) and the administration of the MCD diet was continued for further 4 weeks. Hepatic transcripts of the fibrogenesis markers α1-procollagen and Transforming Growth Factor-β1 (TGF-β1) as evaluated by RT-PCR and staining of hepatic collagen deposition with Sirius Red (magnification 40x). Panels (D-F) The animals were divided to receive AnxA1 (1 µg/daily in saline 5 time a week) (WD+AnxA1) or saline (WD+sal) and the administration of the MCD diet was continued for further 6 weeks. Hepatic transcripts α1-procollagen and TGF-β1 as evaluated by RT-PCR and collagen staining by Sirius Red (magnification 40x). The values refer to 6-8 animals per group and the boxes include the values within 25th and

75th percentile, while the horizontal bars represent the medians. The extremities of the vertical bars (10th-90th percentile) comprise 80% percent of the values.

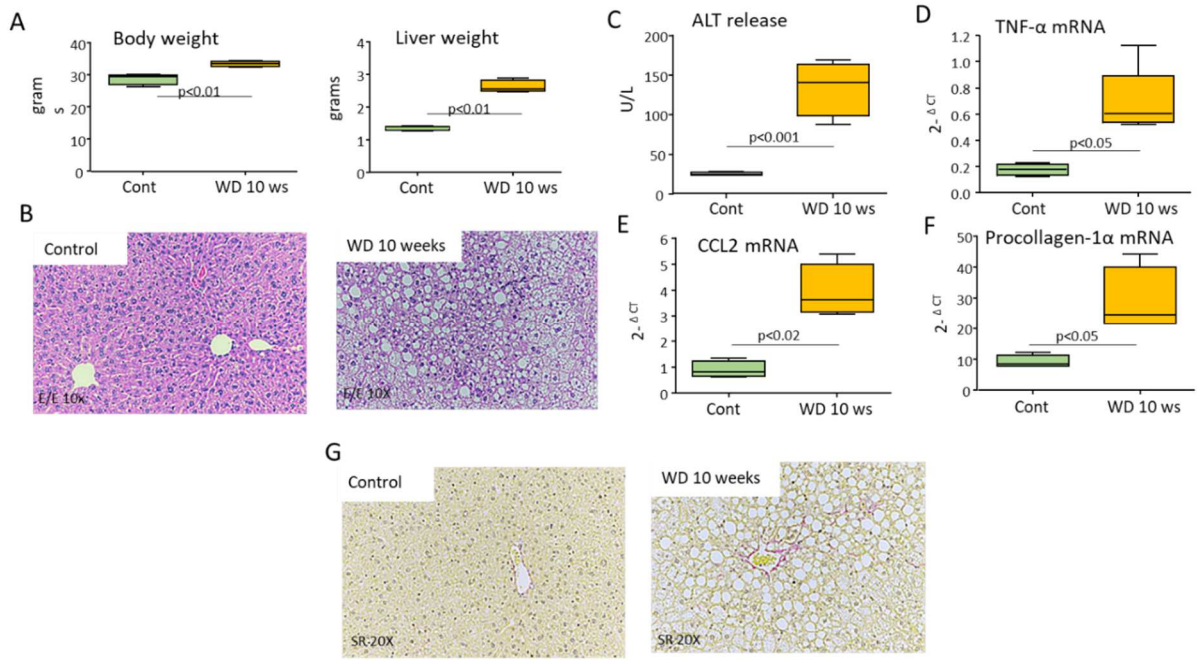

Figure 3: The development of steatohepatitis in mice fed 10 weeks with Western diet (WT).

Wild type C57BL/6 mice receiving WD diet or control chow for 10 weeks were evaluated for the development of NASH. (Panel A) liver and body weights. (Panel B) Hematoxylin/eosin (E/E) staining of liver sections (magnification 10x). (Panels C) Alanine aminotransferase (ALT) release. (Panels D-F) The hepatic mRNA levels of inflammatory markers TNF-α and CD11b and procollagen-1 α as evaluated by RT-PCR. (Panel G) Sirius Red (SR) staining for collagen of liver sections (magnification 20x). The values refer to 4-5 animals per group and the boxes include the values within 25th and 75th percentile, while the horizontal bars represent the medians. The extremities of the vertical bars (10th-90th percentile) comprise 80% percent of the values.

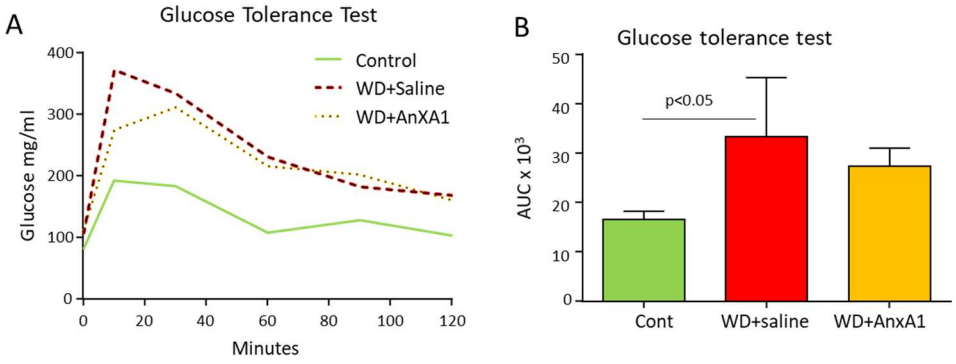

Figure 4: **Annexin A1 (AnxA1) treatment does not improve insulin response in mice receiving Western diet (WT) for 16 weeks.**

NASH was induced in wild type C57BL/6 mice by feeding WD diet for 10 weeks. The animals were then randomly divided in two groups one receiving AnxA1 (1 µg/daily in saline 5 time a week)(WD+AnxA1) and the other the same volume of saline (WD+sal) and the diet was continued for further 6 weeks. (Panel A) Insulin response was evaluated by glucose tolerance test after the intraperitoneal injection of D-glucose (1,5 g/kg body weight). (Panel B) Graphic representation of the area under the curve (AUC) calculated for the glycemic courve. The data refer to 4-5 mice for each experimental group.

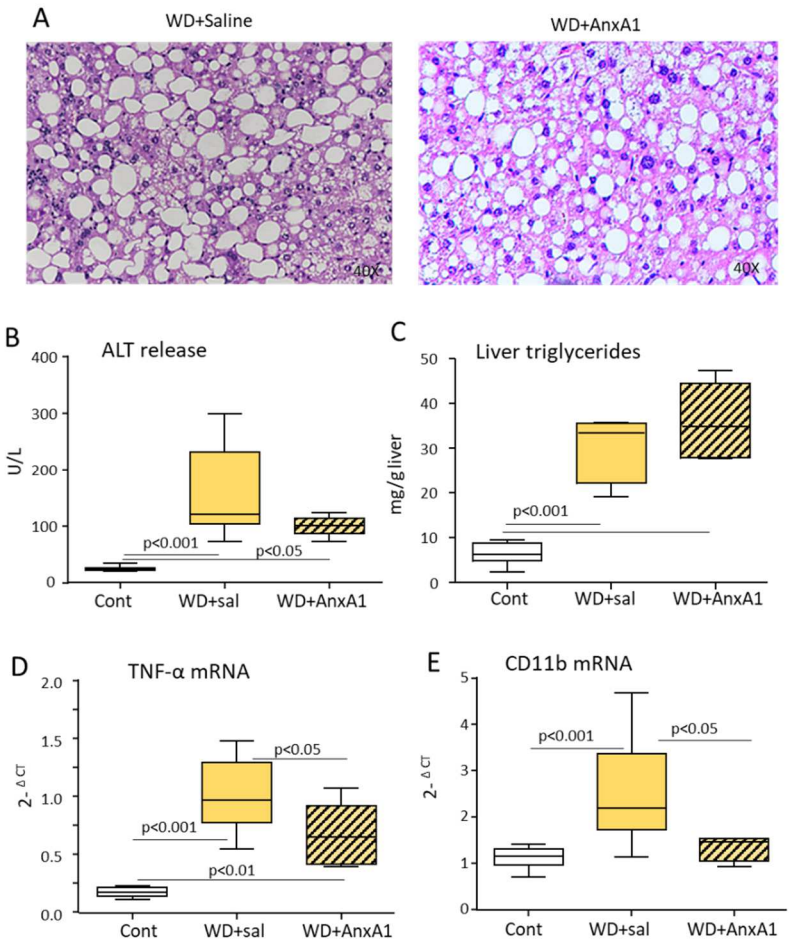

Figure 5: Annexin A1 (AnxA1) supplementation improves steatohepatitis in mice fed with Western diet (WT).

NASH was induced in wild type C57BL/6 mice by feeding WD diet for 10 weeks. The animals were then randomly divided in two groups one receiving AnxA1 (1 µg/daily in saline 5 time a week)(WD+AnxA1) and the other the same volume of saline (WD+sal) and the administration of the diet was continued for further 6 weeks. (Panel A) Hematoxylin/eosin staining of liver sections (magnification 20x). (Panels B,C) Alanine aminotransferase (ALT) release and hepatic triglyceride content. (Panels D-E) The hepatic mRNA levels of inflammatory markers TNF-α and CD11b as evaluated by RT-PCR. The values refer to 5-7 animals per group and the boxes include the values within 25th and 75th percentile, while the horizontal bars represent the medians. The extremities of the vertical bars (10th-90th percentile) comprise 80% percent of the values.

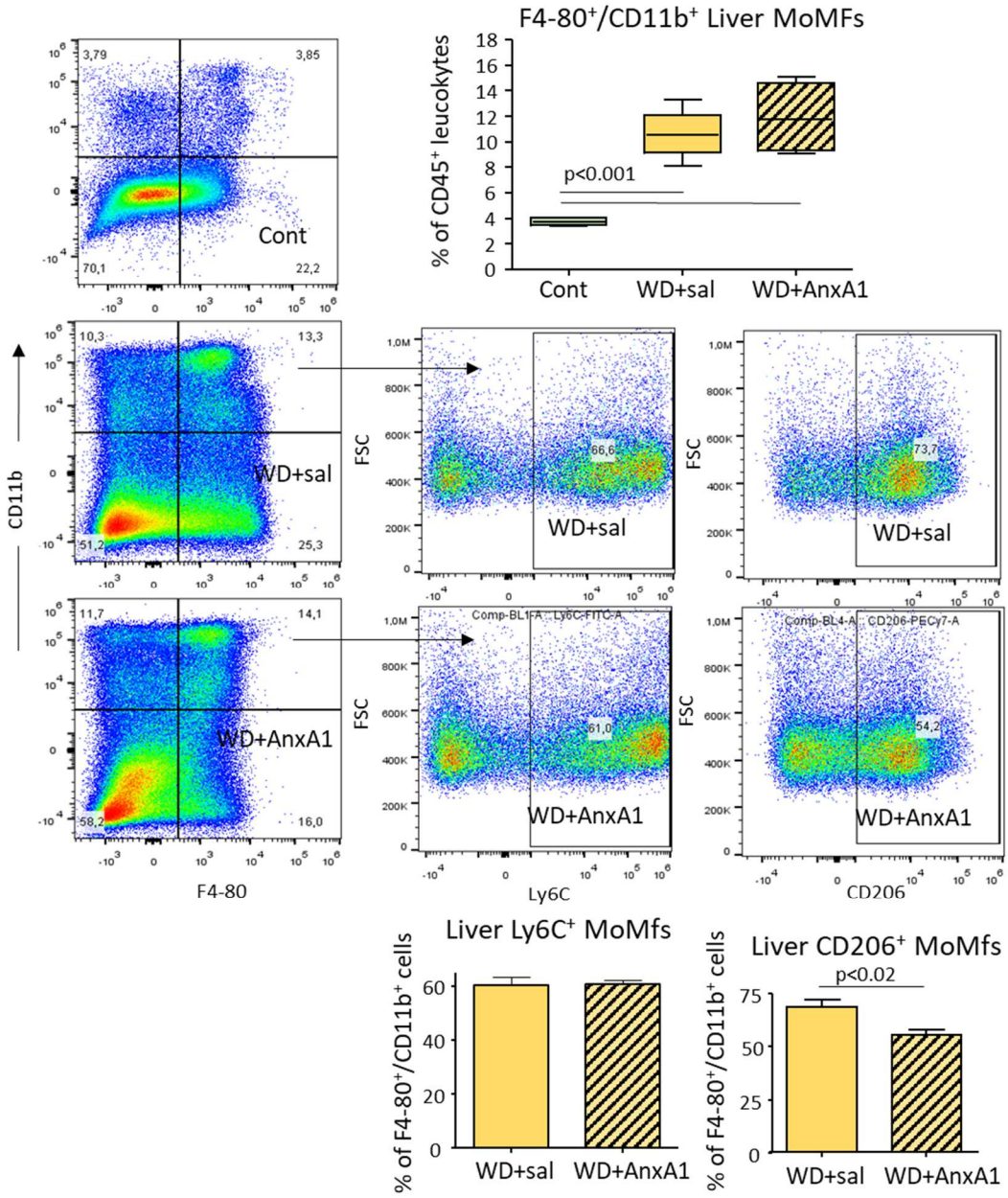

Figure 6: **Effects of Annexin A1 (AnxA1) supplementation on the distribution and features of monocyte-derived macrophages (MoMFs) infiltrating the liver of mice with WD-induced steatohepatitis.**

(Panel A) The intrahepatic distribution of F4-80$^+$/CD11b$^+$ MoMFs and the relative prevalence of cells expressing Ly6C or CD206 was evaluated by flow cytometry in control mice (Cont) or mice receiving WD for 16 weeks in combination with either saline (WD-Sal) or AnxA1 treatment (WD+AnxA1). The values are means ± SD of 3-4 animals for each experimental group.

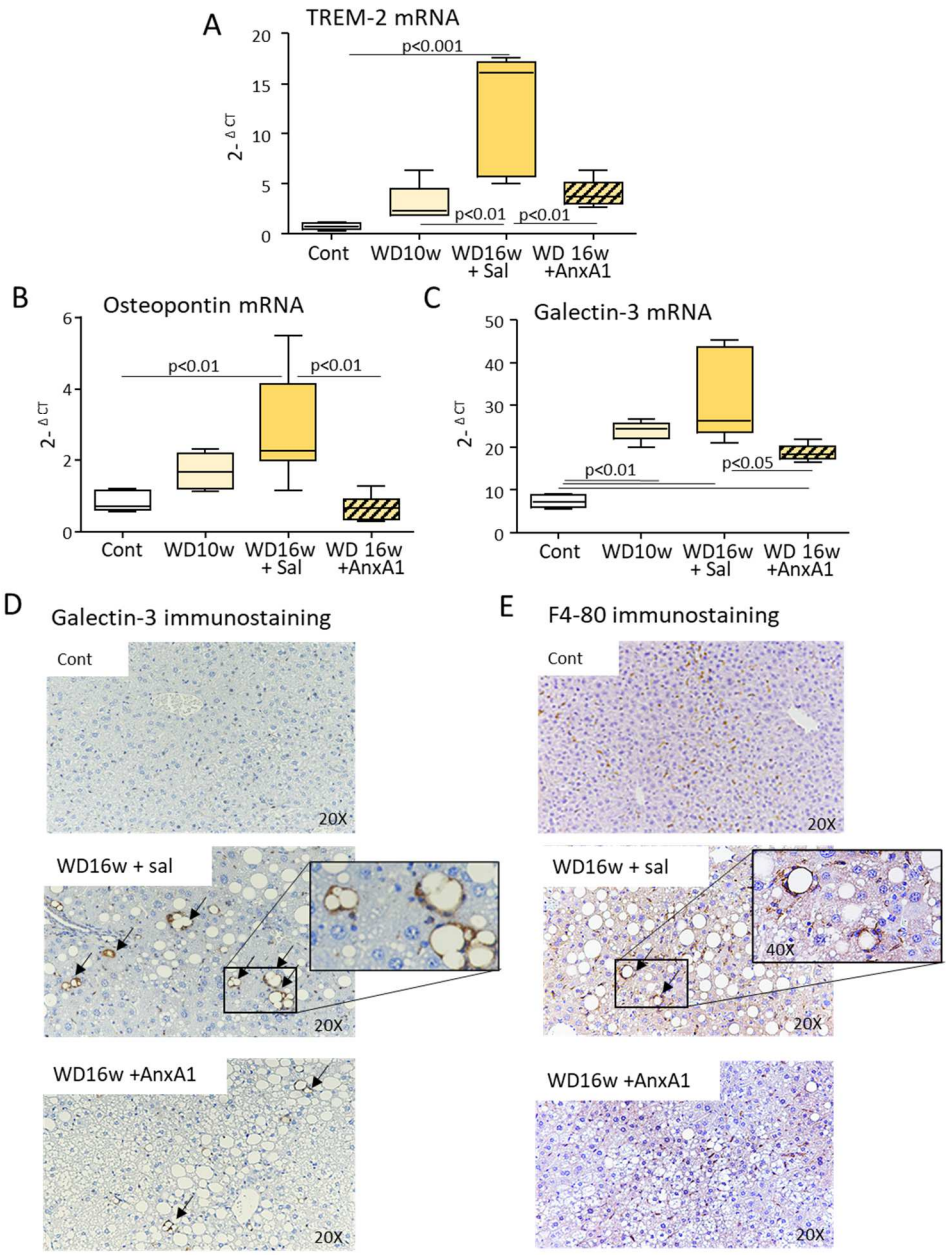

Figure 7: Effects of Annexin A1 (AnxA1) supplementation on hepatic NASH-associated macrophages (NAM).

NASH was induced in wild type C57BL/6 mice by feeding WD diet for 10 weeks. The animals were then randomly divided in two groups one receiving AnxA1 (1 µg/daily in saline 5 time a week)(WD+AnxA1) and the other the same volume of saline (WD+sal) and the diet was continued for further 6 weeks. (Panels A-C) Changes in the hepatic transcripts of NAM markers TREM-2, galectin-3 and ostepontin as evaluated by RT-PCR. (Panels D and E) Liver macrophages immunostaining for galectin-3 and F4-80 (magnification 20x). The inserts show high magnification of the detail of MoMf crown-like structures (arrows). The values refer to 5-7 animals per group and the boxes include the values within 25th and 75th percentile, while the horizontal bars represent the medians. The extremities of the vertical bars (10th-90th percentile) comprise 80% percent of the values.

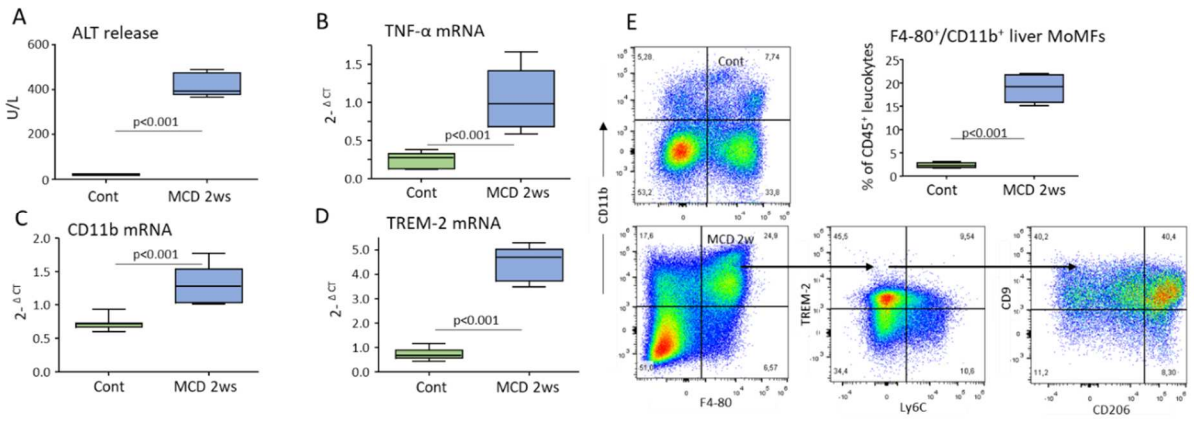

Figure 8: The onset of NASH in mice receiving methionine/choline deficient (MCD) diet parallels with the expansion of TREM-2^{+}/CD9^{+}/CD206^{high} NASH-associated macrophages among liver F4-80^{+}/CD11b^{+} monocyte-derived macrophages (MoMFs).

Wild type C57BL/6 mice receiving either the MCD diet or control chow for 2 weeks were evaluated for the development of steatohepatitis. (Panel A) Alanine aminotransferase (ALT) release. (Panels B-D) The hepatic mRNA levels of inflammatory markers TNF-α and CD11b and TREM-2 as evaluated by RT-PCR. (Panel E) The intrahepatic distribution of F4-80^{+}/CD11b^{+} MoMFs and the relative prevalence of cells expressing Ly6C, TREM-2, CD9 and CD206 was evaluated by flow cytometry. The values refer to 4-5 animals per group and the boxes include the values within 25th and 75th percentile, while the horizontal bars represent the medians. The extremities of the vertical bars (10th-90th percentile) comprise 80% percent of the values.

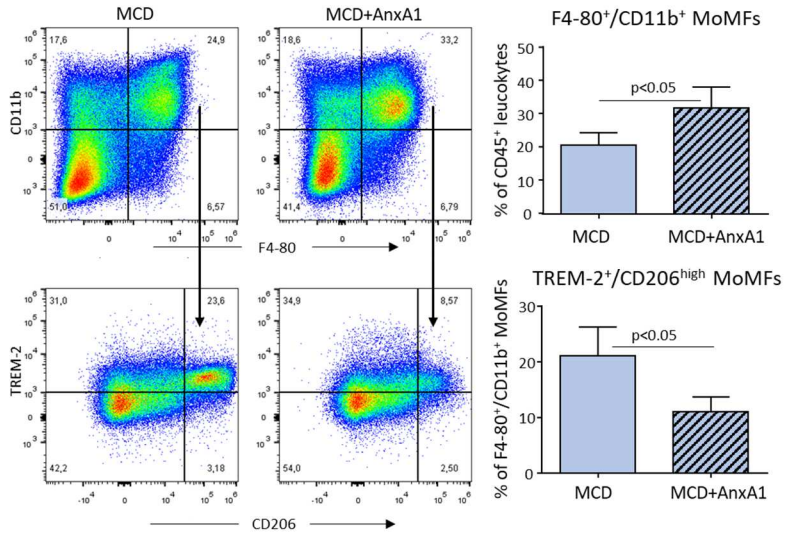

Figure 9: Annexin A1 (AnxA1) supplementation reduces the prevalence of NASH-associated macrophages (NAM) in the livers of mice.

NASH was induced in wild type C57BL/6 mice by feeding MCD diet for 2 weeks and during the second week the animals received for 5 days AnxA1 (1 μg/daily in saline) (MCD+AnxA1) or the same volume of saline (MCD+sal). The intrahepatic distribution of F4-80^{+}/CD11b^{+} MoMFs and the relative prevalence of cells expressing TREM-2

and CD206 was evaluated by flow cytometry. The values are means ± SD of 3-4 animals for each experimental group.

5.4 Discussion

As a result of the endemic presence of over-weight and obesity in the western world, nonalcoholic fatty liver disease (NAFLD) is becoming a leading cause of liver cirrhosis, with the prevalence of NAFLD-related end-stage liver diseases expected to further grow over the next decades (Younossi Z et al. 2018). On this latter respect, a prospective study in more than 400 patients, with biopsy proven NAFLD with or without steatohepatitis, demonstrated that presence of NASH doubles the rate of disease progression to fibrosis (Singh S et al. 2015). Thus, targeting inflammation represents a key aspect for developing effective treatments for progressive NAFLD. In these settings, the interest for a possible therapeutic use of AnxA1 in NASH steams from the observation that the development of insulin resistance, lipid metabolism derangements, lobular inflammation and fibrosis are enhanced in AnxA1-deficient mice receiving either high-fat or MCD diets (Locatelli I et al 2014; Purvis GSD et al. 2019).

By using two different experimental models of NASH, we observe that treating mice with established steatohepatitis with hrAnxA1 not only attenuates liver damage and inflammation but also prevents disease progression to fibrosis. The actions of AnxA1 appear unrelated to effects on metabolic control since, differently from what reported by Purvis and colleagues (Purvis GSD et al. 2019), in our experimental settings hrAnxA1 was ineffective in ameliorating liver steatosis and insulin resistance in mice receiving the WD. Such a discrepancy can be explained by the different experimental models. The high-fat diet used in Purvis' experiments causes a lower degree of hepatic inflammation than the cholesterol-enriched WD used in our work (Wiede F et al. 2018) and this might likely influence the severity of the derangements in lipid and glucose metabolism. Furthermore, the time frame between starting the diet and hrAnxA1 administration, was more than two-fold longer in our protocol, thus entailing the possibility of an at least partially effective recovery from liver fat accumulation.

The ability of AnxA1 to ameliorate NASH hepatic damage and inflammation is in line with its recognized action in reducing granulocyte recruitment and macrophage M1 polarization (Sugimoto MA et al. 2016; Sheikh MH et al. 2018; Locatelli I et al. 2014). Nonetheless, our

results unveil that in NASH AnxA1 is also very effective in preventing disease progression to fibrosis. Such anti-fibrotic action is consistent with previous reports showing that AnxA1 or AnxA1 mimetic peptides improve lung fibrosis induced by bleomycin or silica particles (Trentin PG et al. 2015; Damazo AS et al 2011). In NASH livers, the anti-fibrotic function of hrAnxA1 does not involve changes in the number of hepatic macrophages but it rather associates with the modulation of their phenotype. Treatment with hrAnxA1, in fact, reduces MoMF capacity of forming crown-like aggregates and affects their production of the profibrogenic mediator galectin-3 (Gal-3). In rodents and humans NASH liver, macrophages often form clusters of enlarged and vacuolated cells, known as hepatic crown-like structures or lipogranulomas (Itoh M et al. 2013). Previous studies have shown that these macrophages derive from liver recruited monocytes and display pro-inflammatory activity (Jindhal A et al. 2015; Leroux A et al. 2012; Ioannou GN et al. 2013). In addition, these cells produce mediators which sustain the fibrosis evolution of NASH (Henderson NC et al. 2006; Syn WK et al. 2011) also in view of their colocalization with regions of stellate cell expansion (Remmerie A et al. 2020; Daemen S et al. 2021). So far, the mechanisms leading to the formation of crown-like structures in NASH have not been completely characterized. Studies by Ioannou and coworkers (Horn CL et al.2021) have shown that macrophage phagocytosis of cholesterol crystals present in dying fat-laden hepatocytes promotes the formation of these crown-like structures. It is noteworthy that these macrophages are also the main producers of AnxA1 in both rodent and human NASH livers (Locatelli I et al 2014; Jindal A et al. 2015). However, in NASH patients hepatic AnxA1 transcripts inversely correlate with the severity of fibrosis/cirrhosis [11], while activated hepatic stellate cells co-localize with Gal-3-positive crown-like structures in the livers of AnxA1-deficient mice with NASH (Locatelli I et al. 2014). This opens the strong possibility that endogenous AnxA1 might be involved in a juxtacrine/paracrine loop that regulates macrophage responses to stimuli, which promote crown-like aggregate formation and fibrogenic mediators' secretion.

Recent reports have outlined the heterogeneity of hepatic macrophages in NASH showing that during disease evolution, Kupffer cells are lost, and the liver is enriched by several subsets of MoMFs displaying different phenotypes (Wen Y et al.2021). In more detail, NASH in both rodents and humans is characterized by the abundance of $CD63^{+}/CD9^{+}/GPNMB^{+}/TREM\text{-}2^{+}$ NASH-associated macrophages (NAM) (Itoh M et al. 2013; Xiong X et al. 2019; Seidman JS et

al. 2020; Remmerie A et al. 2020), which are similar to the TREM-2/CD9-expressing lipid-associated macrophages (LAMs) detected in obese adipose tissue (Jaitin D.A et al. 2019) and contribute to the formation of crown-like aggregates (Remmerie A et al. 2020). The work by Ramachandran and co-workers (Jaitin D.A et al. 2019) demonstrated that the TREM-2/CD9/OPN/Gal-3 signature also characterizes scar-associated macrophages identified in human fibrotic livers. Lineage tracking indicates that NAMs and scar-associated macrophages derive from liver infiltrating monocytes (Remmerie A et al. 2020; Ramachandran P et al. 2019) and acquire their phenotype in response to specific signals in interstitial liver niche (Xiong X et al. 2019; Sakai M et al. 2019). We have observed that beside interfering with OPN and Gal-3 gene expression, administration of AnxA1 affects the differentiation of TREM-2^+/$CD9^+$/$CD206^+$ MoMFs, suggesting the possibility that AnxA1 can prevent the development of fibrosis in NASH by reducing their differentiation towards pro-fibrogenic NAMs.

These results unveil a novel functional role for AnxA1 in NASH progression by demonstrating its property of interfering with the development of a specific macrophage phenotype associated with the progression of steatohepatitis to fibrosis. Such a novel function of AnxA1 provides a strong rationale for the application of AnxA1, or AnxA1 analogues, to achieve therapeutic control of NASH evolution.

6. General Discussion

It is increasingly evident that liver infiltrating MoMFs detectable following both acute and chronic damage are highly pleomorphic cells that not only modulate their phenotype shifting from pro-inflammatory to repair macrophages but are also capable to acquire Kupffer cell features (Wen et al. 2021). So far, the complexity of the signals that drive these changes and that makes very heterogeneous the hepatic macrophage pool during chronic liver diseases has only started to be investigated. For instance, the paper by Bonnardel and co-workers (Bonnardel et al. 2019) and Sakai and co-workers (Sakai et al. 2019) have shown that the interaction of MoMFs with sinusoidal endothelial cells (LSECs) and hepatic stellated cells (HSCs) is critical for acquiring a Kupffer cell phenotype. In this setting, the cell contact through Notch 1 receptor with its ligand Delta-like ligand 4 (DLL4) is required for the activation of specific transcription factors, such as Nr1h3, that drive differentiation to Kupffer cells (Bonnardel et al. 2019; Sakai et al. 2019). Beside that the production of colony-stimulating factor 1 (CSF1), transforming growth factor-β1 (TGFβ1) and bone morphogenetic protein (BmP) by LSECs and HSCs along with that of desmosterol by hepatocytes further contribute to this process (Bonnardel et al. 2019; Sakai et al. 2019). Our data indicate additional cross talks can involve T-lymphocytes and particularly CD8+ T-cells that are particularly abundant within the liver. Among such cross talks that mediated by ICOS/ICOSL interaction is particularly important under pathological conditions as it contributes to the survival of Ly6C^{low} reparative MoMFs. It is known that Ly6C^{high} MoMFs have a short life of about 20 hours, while Ly6C^{low} MoMFs can survive for several days (Yona et al. 2013), thus exploiting their functions in clearing death cells and in promoting hepatocyte proliferation and matrix reorganization. At present it is not clear whether this pro-survival action relays on transduction pathway directly depending on ICOSL reverse signalling or involves an enhanced response to other mediators, such as CSF1 which is important for the maintenance of MoMFs. Furthermore, additional studies are required for defining to what extent ICOSL stimulation can contribute to the differentiation of reparative Ly6C^{low} MoMFs since preliminary results indicate that the expression of specific markers as MerTK, TREM2 and CD206 is delayed in peritoneal macrophages obtained by elicitation in ICOSL-deficient mice.

The observation that ICOS/ICOSL dyad represents a novel factor by which $CD8^+$ T-cells influence MoMF functions is important not only for a better understanding of the mechanisms involved in liver repair following acute injury but also for getting new insides in the role of MoMFs in driving hepatic fibrosis in chronic liver diseases. In fact, TREM-2+/ICOSL+ reparative MoMFs show several analogies with scar-associated TREM-2/CD9 recently identified by single cells RNA-sequencing in the livers of human cirrhotic patients (Ramachandran et al. 2019). These cells differentiate from circulating monocytes, have a pro-fibrogenic activity and expand in liver fibrosis (Ramachandran et al. 2019). Interestingly, hepatic MoMFs with a similar phenotype, named NASH-associated macrophages (NAM) have also been recently characterized in either rodent and human NASH and they prevalence correlates with the disease severity and the evolution to fibrosis (). In parallel, the studies concerning NASH have implicated liver cytotoxic $CD8^+$ T-lymphocytes as important players in supporting the disease evolution by showing that $CD8^+$ T-cell ablation effectively ameliorates steatohepatitis (Wolf et al. 2014; Breuer et al. 2020; Plister et al. 2021). Preliminary observations in our laboratory indicate that $CD8^+$ T-cells expanding in NASH express ICOS and that this correlates with a parallel expansion in the number of TREM-2^+/$CD9^+$/$CD206^+$ NAMs which show upregulation of ICOSL. This opens the possibility that $CD8^+$ T-cell activation might be a possible driver for the differentiation/maintenance of NAMs possibly contributing through this mechanism to the disease evolution to fibrosis.

Our studies using experimental models of NASH have also shown that the pro-fibrogenic action of NAMs can be modulated by annexin A1 (AnxA1). Studies by our laboratory have previously shown the induction of NASH in AnxA1-deficient mice was characterized by an enhanced macrophage recruitment and a stimulation in their pro-inflammatory and pro-fibrogenic activities (Locatelli et al. 2014). Conversely, the in vitro addition of recombinant AnxA1 to macrophages isolated from NASH livers reduced their pro-inflammatory activity by stimulating the production of interleukin-10 (Locatelli et al. 2014). The present data add on this aspect, by showing that AnxA1 supplementation of mice prevent NASH progression to fibrosis through an interference with NAM phenotype. We have in fact observed that AnxA1 affects the formation of macrophage crown-like aggregates, which relay on the presence of NAMs (Remmerie et al. 2020; Daemen et al. 2021) and reduces the expression of NAM markers such as TREM-2, Gal-3 and OPN. Since the overall liver prevalence

of MoMF is not influenced by AnxA1 it is presently unclear whether these changes are due the block of NAM differentiation or a stimulus for a further differentiation leading to a Kupffer cell-like phenotype, as recently proposed by Daemen and coworkers (Daemen et al. 2021). Further experiments are ongoing to specifically address this point and to define possible interactions between ICOSL and AnxA1 signaling in modulating NAM features. It is noteworthy, that the modulation of NAM phenotype induced by AnxA1 involve the reduction in the production of Gal-3 by MoMFs in crown-like aggregates. This is consistent with previous observation by Locatelli and co-workers who reported that the worsening of fibrosis AnxA1-deficient mice associates with a marked upregulation in liver Gal-3 by aggregates containing MoMFs and activated HSCs (Locatelli et al. 2014). Gal-3 is a member of the galectin family, a group of lectins that participates in the regulation of cell adhesion, proliferation, and survival, as well as in the modulation of tissue inflammation and fibrosis (Henderson and Sethi 2009). On this latter respect, Gal-3 secretion by macrophages has been implicated in the promotion of renal fibrosis (Henderson et al. 2008), whereas genetic deletion or inhibition of Gal-3 attenuates HSC activation and hepatic collagen deposition in experimental models of chronic liver diseases (Traber et al. 2013; Traber and Zomer 2013). Such a role of AnxA1 in regulating Gal-3 is a further indication that it's signalling specifically can impact on the phenotype of MoMFs involved in tissue repair.

In conclusion, the data obtained during my doctoral training have given new evidence on the complexity of the mechanisms involved in regulating MoMF plasticity during the evolution of liver damage pointing to the importance of the combination of either released mediators and specific cellular interactions in modulating cell phenotype and functions. Targeting these interactions might offer the possibility for developing novel therapeutic approaches to both acute and chronic liver diseases.

7. References

- Amstrong MJ, Adams LA, Canbay A et al. Extrahepatic complications of non-alcoholic fatty liver disease. Hepatol 59:1174-1197 (2014).
- Arts RJ, Joosten LA, van der Meer JW, Netea MG et al. TREM-1: intracellular signaling pathways and interaction with pattern recognition receptors. J Leukoc Biol93:209-215 (2013).
- Baeck, C. et al. Pharmacological inhibition of the chemokine C-C motif chemokine ligand 2 (monocyte chemoattractant protein 1) accelerates liver fibrosis regression by suppressing Ly-6C (+) macrophage infiltration in mice. Hepatology 59, 1060–1072 (2014).
- Beattie, L. et al. Bone marrow-derived and resident liver macrophages display unique transcriptomic signatures but similar biological functions. J. Hepatol. 65, 758–768 (2016).
- Bennett H, Troutman TD, Sakai M, Glass CK. Epigenetic Regulation of Kupffer Cell Function in Health and Disease. Front Immunol.11 (2021).
- Bernal W et al. Acute liver failure. N Engl J Med 369:2525-2534 (2013).
- Bonnardel, J. et al. Stellate Cells, Hepatocytes, and Endothelial Cells Imprint the Kupffer Cell Identity on Monocytes Colonizing the Liver Macrophage Niche. Immunity 51, 638–654 e9 (2019).
- Bosurgi, L. et al. Macrophage function in tissue repair and remodeling requires IL-4 or IL-13 with apoptotic cells. Science 356, 1072–1076 (2017).
- Boulter L, Govaere O, Bird TG, Radulescu S, Ramachandran P, Pellicoro A, et al. Macrophage-derived Wnt opposes Notch signaling to specify hepatic progenitor cell fate in chronic liver disease. Nat Med 18:572-579 (2012).
- Breuer DA, Pacheco MC, Washington MK, et al. $CD8^+$ T cells regulate liver injury in obesity-related nonalcoholic fatty liver disease. Am J Physiol Gastrointest Liver Physiol. 318: G211-G224 (2019).
- Cho Y, Szabo G. Two faces of neutrophils in liver disease development and progression. Hepatol 74:503-512 (2021)
- Coelho I, Duarte N, Barros A, Macedo MP, Penha-Gonçalves C. Trem-2 promotes emergence of restorative macrophages and endothelial cells during recovery from hepatic tissue damage. Front Immunol 11:616044 (2021).
- Daemen S, Gainullina A, et al.Dynamic Shifts in the Composition of Resident and Recruited Macrophages Influence Tissue Remodeling in NASH. Cell Rep 34:108626 (2021).
- Dal-Secco D, Wang J, Zeng Z, et al. A dynamic spectrum of monocytes arising from the in situ reprogramming of CCR21 monocytes at a site of sterile injury. J Exp Med 212:447-456 (2015).
- Damazo AS et al.Endogenous annexin A1 counter-regulates bleomycin-induced lung fibrosis. BMC Immunol Oct 19; 12:59 (2011).
- Deppermann, C. et al. Macrophage galactose lectin is critical for Kupffer cells to clear aged platelets. J. Exp. Med. 217, e20190723 (2020).
- Dudek M, Pfister D, Donakonda S, et al. Auto-aggressive CXCR6 + CD8 T cells cause liver immune pathology in NASH. Nature 592:444-449(2021).
- Doherty D.G, Antigen-presenting cell function in the tolerogenic liver environment. J Autoimmun 66:60-75. (2016).
- Dianzani C, Minelli R, et al. B7h triggering inhibits umbilical vascular endothelial cell adhesiveness to tumor cell lines and polymorphonuclear cells. J. Immunol 185:3970–3979 (2010).
- Dianzani C, Minelli R, et al. B7h triggering inhibits the migration of tumor cell lines. J. Immunol192:4921–4931 (2014).
- Ehling, J. et al. CCL2-dependent infiltrating macrophages promote angiogenesis in progressive liver fibrosis. Gut 63, 1960–1971 (2014).
- Holt, M. P., Cheng, L. & Ju, C. Identification, and characterization of infiltrating macrophages in acetaminophen-induced liver injury. J. Leukoc. Biol. 84, 1410–1421 (2008).

- Geissmann F, Jung S, Littman DR et al. Blood monocytes consist of two principal subsets with distinct migratory properties. Immunity 19:71-82(2003).
- Gigliotti CL, Boggio E, Clemente N, et al. ICOS-Ligand Triggering Impairs Osteoclast Differentiation and Function In Vitro and In Vivo. J Immunol 197:3905-3916 (2016).
- Girgis, N. M. et al. Ly6C(high) monocytes become alternatively activated macrophages in schistosome granulomas with help from CD4+ cells. PLoS Pathog. 10 (2014).
- Guilliams M. et al. Unsupervised high-dimensional analysis aligns dendritic cells across tissues and species. *Immunity* **45**, 669–684 (2016).
- Gomez Perdiguero, E. et al. Tissue-resident macrophages originate from yolksac-derived erythro-myeloid progenitors. Nature 518, 547–551 (2015).
- Helmy, K. Y. et al. CRIg: a macrophage complement receptor required for phagocytosis of circulating pathogens. Cell 124, 915–927 (2006).
- Henderson NC, Mackinnon AC, et al. Galectin-3 regulates myofibroblast activation and hepatic fibrosis. Proc. Natl Acad. Sci. USA 103:5060–5065 (2006).
- Henderson NC, Sethi T et al. The regulation of inflammation by galectin-3. Immunol Rev 230:160-171(2009).
- Henderson NC, Mackinnon AC, et al. Galectin-3 expression and secretion links macrophages to the promotion of renal fibrosis. Am J Pathol 172:288-298(2008).
- Heymann, F. et al. Liver inflammation abrogates immunological tolerance induced by Kupffer cells. Hepatology 62, 279–291 (2015).
- Heymann, F. & Tacke, F et al. Immunology in the liver-from homeostasis to disease. Nat. Rev. Gastroenterol. Hepatol. 13, 88–110 (2016).
- Holt, M. P., Cheng, L. & Ju, C. Identification and characterization of infiltrating macrophages in acetaminophen-induced liver injury. J. Leukoc. Biol. 84, 1410–1421 (2008).
- Horn CL, Morales AL.Role of Cholesterol-Associated Steatohepatitis in the Development of NASH. Hepatol Commun (2021).
- Ioannou, G.N., Haigh, W.G, et al., 2013. Hepatic cholesterol crystals and crown-like structures distinguish NASH from simple steatosis. J. Lipid Res. 54,1326–1334 (2013).
- Itoh M, Kato H, et al. Hepatic crown-like structure: a unique histological feature in non-alcoholic steatohepatitis in mice and humans.One 8:e82163. (2013).
- Jaeschke H, Ramachandran A et al. Mechanisms and pathophysiological significance of sterile inflammation during acetaminophen hepatotoxicity. Food Chem Toxicol 138:111240 (2020)
- Jaitin, D.A, Adlung, L, Deczkowska, A et al. Lipid-Associated Macrophages Control Metabolic Homeostasis in a Trem2-Dependent Manner. Cell;178, 686–698 (2019).
- Jindal A, Bruzzì S, Sutti S, Locatelli I, Bozzola C, Paternostro C, Parola M, Albano E. Fat-laden macrophages modulate lobular inflammation in nonalcoholic steatohepatitis (NASH). Exp Mol Pathol 99:155-162. (2015)
- Karlmark, K. R. et al. Hepatic recruitment of the inflammatory Gr1+ monocyte subset upon liver injury promotes hepatic fibrosis. Hepatology 50, 261–274 (2009).
- Karlmark KR, et al. The fractalkine receptor CX_3CR1 protects against liver fibrosis by controlling differentiation and survival of infiltrating hepatic monocytes. Hepatol.52:1769-1782. (2010).
- Ke B, Shen XD, et al. The CD154-CD40 T-cell co-stimulation pathway in liver ischemia and reperfusion inflammatory responses Transplantation79:1078-1083 (2005).
- Khandoga A, et al. CD4+ T cells contribute to postischemic liver injury in mice by interacting with sinusoidal endothelium and platelets Hepatol 43:306-315 (2006).
- Kim, K. W, Zhang, N et al. Homegrown Macrophages. Immunity 45, 468–470 (2016).
- Koh KH, Cao Y et al. Nonimmune cell-derived ICOS ligand functions as a renoprotective αvβ3 integrin-selective antagonist. J Clin Invest129:1713-1726 (2019)
- Krenkel O et al. Therapeutic inhibition of inflammatory monocyte recruitment reduces steatohepatitis and liver fibrosis. Hepatology 67, 1270–1283 (2018).
- Krenkel O. & Tacke, F et al. Liver macrophages in tissue homeostasis and disease. Nat. Rev. Immunol. 17, 306–321 (2017).
- Kruger, A. J. et al. Prolonged cenicriviroc therapy reduces hepatic fibrosis despite steatohepatitis in a diet-induced mouse model of nonalcoholic steatohepatitis. Hepatol. Commun. 2, 529–545 (2018).
- Kubes P, Mehal WZ et al. Sterile inflammation in the liver. Gastroenterology. 143:1158-1172 (2012).

- Kusters DHM et al.Pharmacological Treatment with Annexin A1 Reduces Atherosclerotic Plaque Burden in LDLR-/- Mice on Western Type Diet. PLoS ONE 10 e0130484 (2015).
- Lau JKC, Zhang X and Yu J et al. Animal models of non-alcoholic fatty liver disease: current perspectives and recent advances. J Pathol; 241: 36–44 (2017).
- Lee, J. H. et al. Mitochondrial double-stranded RNA in exosome promotes interleukin-17 production through toll-like receptor 3 in alcoholic liver injury. Hepatology. 72, 609–625 (2020).
- Leroux A et al. Toxic lipids stored by Kupffer cells correlates with their pro-inflammatory phenotype at an early stage of steatohepatitis. J Hepatol 57:141-149(2012).
- Liaskou, E et al. Monocyte subsets in human liver disease show distinct phenotypic and functional characteristics. Hepatology 57, 385–398 (2013).
- Li DY et al. ICOS+ Tregs: A Functional Subset of Tregs in Immune Diseases. Front Immunol 11:2104 (2020).
- Li Z, Zhao et al. FOXO3-dependent apoptosis limits alcohol-induced liver inflammation by promoting infiltrating macrophage differentiation. Cell Death Discov. 4, 16 (2018).
- Lindenmeyer CC, McCullough AJ. The natural history of non-alcoholic fatty liver disease -an evolving view. Clin. Liver 22:11–21 (2018).
- Liu X, Quan N. Immune Cell Isolation from Mouse Femur Bone Marrow. Bio Protoc 20:5 (2015).
- Locatelli I, Sutti, S. Endogenous annexin A1 is a novel protective determinant in non-alcoholic steatohepatitis in mice. Hepatol 60:531–544 (2014).
- MacParland, S. A. et al. Single cell RNA sequencing of human liver reveals distinct intrahepatic macrophage populations. Nat. Commun. 9, 4383 (2018).
- Maeda S, et al. Inducible costimulator (ICOS) and ICOS ligand signaling has pivotal roles in skin wound healing via cytokine production. Am J Pathol 179:2360–2369 (2011).
- Marra, F. & Tacke, F et al. Roles for chemokines in liver disease. Gastroenterology 147, 577–594.e1 (2014).
- McArthur S, Annexin A1 drives macrophage skewing to accelerate muscle regeneration through AMPK activation. J Clin Invest 130:1156-1167(2020).
- McDonald B, et al. Innate Immune Cell Trafficking and Function During Sterile Inflammation of the Liver. Gastroenterol. 151:1087-1095 (2016).
- Michalopoulos GK, Bhushan B, et al. Liver regeneration: biological and pathological mechanisms and implications. Nat Rev Gastroenterol Hepatol 18:40-55 (2021).
- Montrief T, et al. Long B. Acute liver failure: A review for emergency physicians. Am J Emerg Med 37:329-337 (2019).
- Mossanen, J. C. et al. Chemokine (C-C motif) receptor 2-positive monocytes aggravate the early phase of acetaminophen-induced acute liver injury. Hepatology 64, 1667–1682 (2016).
- Nguyen-Lefebvre AT, Ajith A, et al. The innate immune receptor TREM-1 promotes liver injury and fibrosis. J Clin Invest 128:4870-4883 (2018).
- Occhipinti S, Dianzani C, Chiocchetti A, Boggio, Clemente N, Gigliotti C L, et al. Triggering of B7h by the ICOS modulates maturation and migration of monocyte-derived dendritic cells. J Immunol 190:1125-1134 (2013).
- Pallett LJ, et al. IL-2(high) tissue-resident T cells in the human liver: sentinels for hepatotropic infection. J Exp Med 214:1567-1580. (2017).
- Perugorria MJ et al. Non-parenchymal TREM-2 protects the liver from immune-mediated hepatocellular damage. Gut 68:533-546 (2019).
- Pfister, D. Gonzalo Núñez N, Pinyolet R, et al. NASH limits anti-tumour surveillance in immunotherapy-treated HCC. Nature 592:450–456(2021).
- Puengel T, Krenkel O, et al. Differential impact of the dual CCR2/CCR5 inhibitor cenicriviroc on migration of monocyte and lymphocyte subsets in acute liver injury. PLoS One 12 (2017).
- Purvis GSD et al. Identification of AnnexinA1 as an Endogenous Regulator of RhoA, and Its Role in the Pathophysiology and Experimental Therapy of Type-2 Diabetes. Front Immunol 27:10:571 (2019).
- Ramachandran, P. et al. Differential Ly-6C expression identifies the recruited macrophage phenotype, which orchestrates the regression of murine liver fibrosis. Proc. Natl Acad. Sci. USA 109, E3186–E3195 (2012).
- Ramachandran P, Dobie R et al. Resolving the fibrotic niche of human liver cirrhosis at single cell level. Nature. 575: 512–518. (2019).

- Ratziu, V. et al. Cenicriviroc Treatment for adults with non-alcoholic steatohepatitis and fibrosis: final analysis of the phase 2b CENTAUR Study. Hepatology.72, 892–905 (2020).
- Reimer KC, Wree A, Roderburg C, Tacke F et al. new drugs for NAFLD: lessons from basic models to the clinic. Hepatol Int. 14:8-23(2020).
- Remmerie A, Thoné T et al. Osteopontin Expression Identifies a Subset of Recruited Macrophages Distinct from Kupffer Cells in the Fatty Liver. Immunity 53, 641–657 (2020).
- Remmerie A. Scott C.L et al Macrophages and lipid metabolism. Cell Immunol 10.1016 (2018).
- Rotman Y, Sanyal AJ et al. Current and upcoming pharmacotherapy for non-alcoholic fatty liver disease. Gut 66:180-190 (2017).
- Saha, B. et al. Extracellular vesicles from mice with alcoholic liver disease carry a distinct protein cargo and induce macrophage activation through heat shock protein 90. Hepatology 67, 1986–2000 (2018).
- Sakai M. et al. Liver-Derived Signals Sequentially Reprogram Myeloid Enhancers to Initiate and Maintain Kupffer Cell Identity. Immunity 51, 655–670 e8 (2019).
- Santhekadur PK, Kumar DP et al. Preclinical models of non-alcoholic fatty liver disease. J Hepatol 68:230-237 (2018).
- Scott, C. L. & Guilliams, M.et al. The role of Kupffer cells in hepatic iron and lipid metabolism. J. Hepatol. 69, 1197–1199 (2018).
- Seidman JS, Troutman et al. TD Niche-Specific Reprogramming of Epigenetic Landscapes Drives Myeloid Cell Diversity in Nonalcoholic Steatohepatitis. Immunity 52:1057-1074 (2020).
- Serhan CN, et al. Treating inflammation and infection in the 21st century: new hints from decoding resolution mediators and mechanisms. FASEB J. 31:1273-1288 (2017)
- Shapiro, H., Pecht, T., Shaco-Levy, R., et al. Adipose tissue foam cells are present in human obesity. J. Clin. Endocrinol. Metab. 98, 1173–1181(2013).
- Sheikh MH, Solito E. Annexin A1: Uncovering the Many Talents of an Old Protein. Int J Mol Sci. 19:1045 (2018).
- Singh S et al. Fibrosis progression in nonalcoholic fatty liver vs nonalcoholic steatohepatitis: a systematic review and meta-analysis of paired-biopsy studies Clin Gastroenterol Hepatol 13:643-654 (2015).
- Sierro, F, et al. A Liver Capsular Network of Monocyte-Derived Macrophages Restricts Hepatic Dissemination of Intraperitoneal Bacteria by Neutrophil Recruitment. Immunity 47, 374–388 e6 (2017).
- Stutchfield, B. M. et al. CSF1 restores innate immunity after liver injury in mice and serum levels indicate outcomes of patients with acute liver failure. Gastroenterology 149, 1896–1909.e14 (2015).
- Sugimoto MA, Vago JP, Teixeira MM, Sousa LP et al. Annexin A1 and the Resolution of Inflammation: Modulation of Neutrophil Recruitment, Apoptosis, and Clearance. J Immunol Res 2016:8239258 (2016).
- Sutti S, Albano E, et al. Adaptive immunity: an emerging player in the progression of NAFLD. Nat Rev Gastroenterol Hepatol.17:81-92 (2020).
- Sutti S C, Albano E, et al. CX3CR1 modulates the anti-inflammatory activity of hepatic dendritic cells in response to acute liver injury. Clin Sci 131:2289-2301 (2017).
- Syn WK, Choi SS, Liaskou E, et al. Osteopontin is induced by hedgehog pathway activation and promotes fibrosis progression in nonalcoholic steatohepatitis. Hepatol 53:106-115 (2011).
- Szabo, G. & Csak, T et al. Inflammasomes in liver diseases. J. Hepatol. 57, 642–654 (2012).
- Tacke, F. & Trautwein, C et al. Mechanisms of liver fibrosis resolution. J. Hepatol. 63, 1038–1039 (2015).
- Tacke, F. & Zimmermann H et al. W. Macrophage heterogeneity in liver injury and fibrosis. J. Hepatol. 60, 1090–1096 (2014).
- Tang G, Qin Q et al. Reverse signaling using an inducible costimulator to enhance immunogenic function of dendritic cells. Cell. Mol. Life Sci 66:3067–3080 (2009).
- Terpstra, V. & van Berkel, T. J et al. Scavenger receptors on liver Kupffer cells mediate the in vivo uptake of oxidatively damaged red blood cells in mice. Blood 95,2157–2163 (2000).
- Traber PG, Chou H et al. Regression of fibrosis and reversal of cirrhosis in rats by galectin inhibitors in thioacetamide-induced liver disease. PLoS One;8:e75361(2013).
- Trentin PG et al. Annexin A1 mimetic peptide controls the inflammatory and fibrotic effects of silica particles in mice. Br J Pharmacol 172:3058-3071 (2015).
- Triantafyllou, E. et al. MerTK expressing hepatic macrophages promote the resolution of inflammation in acute liver failure. Gut 67, 333–347 (2018).
- Tsochatzis EA, Bosch J, Burroughs AK et al. Liver cirrhosis. Lancet.383:1749-61 (2014).

- Wahl Ch, Bochtler P, Chen L et al. B7-H1 on hepatocytes facilitates priming of specific CD8 T cells but limits the specific recall of primed responses. Gastroenterol 135:980 -988 (2008).
- Wang, J. & Kubes, P et al. A Reservoir of Mature Cavity Macrophages that Can Rapidly Invade Visceral Organs to Affect Tissue Repair. Cell 165, 668–678 (2016).
- Wehr A. et al. Chemokine receptor CXCR6-dependent hepatic NK T Cell accumulation promotes inflammation and liver fibrosis. J. Immunol. 190, 5226–5236 (2013).
- Wen Y, et al. Hepatic macrophages in liver homeostasis and diseases-diversity, plasticity, and therapeutic opportunities. Cell Mol Immunol 18:45-56 (2021)
- Weston CJ, Zimmermann HW, Adams DH et al. The Role of Myeloid-Derived Cells in the Progression of Liver Disease Front. Immunol., 10:893.
- Wiede F, Tiganis T et al. Isolation and Characterization of Mouse Intrahepatic Lymphocytes by Flow Cytometry. Methods Mol Biol 1725:301-311 (2018).
- Wikenheiser DJ, Stumhofer JS et al. ICOS co-stimulation: Friend or foe? Front Immunol 7:304 (2016).
- Williams CD et al. Neutrophil activation during acetaminophen hepatotoxicity and repair in mice and humans. Toxicol. Appl.Pharmacol275:122–133 (2014)
- Willekens, F. L. et al. Liver Kupffer cells rapidly remove red blood cell-derived vesicles from the circulation by scavenger receptors. Blood 105, 2141–2145 (2005).
- Wolf MJ, et al. Metabolic activation of intrahepatic CD8+ T cells and NKT cells causes nonalcoholic steatohepatitis and liver cancer via cross-talk with hepatocytes. Cancer Cell;26:549-564 (2014).
- Wu L et al. Annexin A1 alleviates kidney injury by promoting the resolution of inflammation in diabetic nephropathy. Kidney Int 100:107-121 (2021).
- Xerox A, Ferrere G, et al. Toxic lipids stored by Kupffer cells correlates with their pro-inflammatory phenotype at an early stage of steatohepatitis. J Hepatol. 57: 141-149 (2012).
- Xiong X, Kuang H et al. Landscape of Intercellular Crosstalk in Healthy and NASH Liver Revealed by Single-Cell Secretome Gene Analysis. Mol Cell. 75:644-660 (2019).
- Yan ML., Wang YD, et al. Inhibition of allogeneic Tcell response by Kupffer cells expressing indoleamine 2,3-dioxygenase. World J. Gastroenterol. 16, 636–640 (2010).
- Yan J, Li S, et al. The role of the liver in sepsis. Int. Rev. Immunol. 33, 498–510 (2014).
- Yang W, et al. Neutrophils promote the development of reparative macrophages mediated by ROS to orchestrate liver repair. Nat. Commun. 10, 1076 (2019).
- Yona, S. et al. Fate mapping reveals origins and dynamics of monocytes and tissue macrophages under homeostasis. Immunity 38, 79–91 (2013).
- Younes R, Bugianesi E, et al. Should we undertake surveillance for HCC in patients with NAFLD? J Hepatol.68:326-334. (2018).
- Younossi Z, Anstee QM, Marietti M, et al. Global burden of NAFLD and NASH: trends, predictions, risk factors and prevention. Nat Rev Gastroenterol Hepatol.15:11-20 (2018)
- You Q., Cheng L et al. Mechanism of T cell tolerance induction by murine hepatic Kupffer cells. Hepatology 48, 978–990 (2008).
- You Q, Holt M et al. Role of hepatic resident and infiltrating macrophages in liver repair after acute injury. Biochem Pharmacol 86:836-843 (2013).
- Zhang C, et al. 'Repair' Treg Cells in Tissue Injury. Cell Physiol Biochem 43:2155-2169 (2017).
- Zheng H, Jia L, et al. TREM2 Promotes Microglial Survival by Activating Wnt/b-Catenin Pathway. J Neurosci 37:1772–1784 (2017).
- Zigmond E, Samia-Grinberg S, Pasmanik-Chor M, Brazowski E, Shibolet O, Halpern Z, et al. Infiltrating monocyte-derived macrophages and resident kupffer cells display different ontogeny and functions in acute liver injury. J Immunol 193:344-353 (2014).
- Zwacka RM, et al. CD4(+) T-lymphocytes mediate ischemia/reperfusion-induced inflammatory responses in mouse liver. J Clin Invest 100:279-289 (1997).

Acknowledgement

Firstly, I would like to express my sincere gratitude to my advisor **Prof. Emanuele Albano** for his immense knowledge and plentiful experience have encouraged me in all the time of my academic research and daily life. I could not have imagined having a better advisor and mentor for my Ph.D. study. I would also like to thank Asst. Prof. Salvatore Sutti who supported towards scientific research. I would like to thank lab mates, colleagues, and research team –Naresh Naik Ramavath, Alessia Provera, Suguna Reddy, Simone Fiorella, Antonio, Carmen for a cherished time spent together in the lab. Finally, I must express my very profound gratitude and special thanks to **Professor Georgio Bellomo** for encouraging me.